UNIVERSITÀ POLITECNICA DELLE MARCHE
Repository ISTITUZIONALE

Effect of alloying elements on the properties of Ti-Al-Si alloys prepared by powder metallurgy

This is the peer reviewd version of the followng article:

Original
Effect of alloying elements on the properties of Ti-Al-Si alloys prepared by powder metallurgy / Knaislová, A., Šimůnková, V., Novák, P., Průša, F., Cabibbo, M., Jaworska, L., Vojtěch., D.. - In: JOURNAL OF ALLOYS AND COMPOUNDS. - ISSN 0925-8388. - ELETTRONICO. - 868:(2021). [10.1016/j.jallcom.2021.159251]

Availability:
This version is available at: 11566/291511 since: 2024-04-11T14:29:52Z

Publisher:

Published
DOI:10.1016/j.jallcom.2021.159251

Terms of use:

The terms and conditions for the reuse of this version of the manuscript are specified in the publishing policy. The use of copyrighted works requires the consent of the rights' holder (author or publisher). Works made available under a Creative Commons license or a Publisher's custom-made license can be used according to the terms and conditions contained therein. See editor's website for further information and terms and conditions.
This item was downloaded from IRIS Università Politecnica delle Marche (https://iris.univpm.it). When citing, please refer to the published version.

(Article begins on next page)

25 October 2026

Journal of Alloys and Compounds

Effect of alloying elements on the properties of Ti-Al-Si alloys prepared by powder metallurgy

--Manuscript Draft--

Manuscript Number:	JALCOM-D-20-14806R2
Article Type:	Full Length Article
Keywords:	Intermetallics; mechanical alloying; sintering; Microstructure; Mechanical properties; oxidation
Corresponding Author:	Anna Knaislová University of Chemistry and Technology, Prague Prague 6, CZECH REPUBLIC
First Author:	Anna Knaislová, Dr.
Order of Authors:	Anna Knaislová, Dr.
	Vendula Šimůnková, Ing.
	Pavel Novák, assoc. prof.
	Filip Průša, Dr.
	Marcello Cabibbo, assoc. prof.
	Lucyna Jaworska, prof.
	Dalibor Vojtěch, prof.
Abstract:	Intermetallic alloys based on Ti-Al-Si system are significant for their excellent high-temperature properties, especially for resistance against oxidation and for achieving good mechanical properties at elevated temperatures. The main problem of these materials is high brittleness at room temperature. In the previous work, selected alloying elements were added into the Ti-Al-Si alloys prepared by reactive sintering, but the properties did not meet the requirements for subsequent use in the automotive or aerospace industry, since the materials had a very porous microstructure. Here, the addition of cobalt, chromium, iron, molybdenum, niobium and nickel into the TiAl15Si15 alloy prepared by mechanical alloying and Spark Plasma Sintering is tested and it is expected to improve the mechanical and high-temperature properties. In this paper, the Ti-Al-Si alloys have been assessed on basis of microstructure, phase composition, mechanical and tribological properties, such as hardness, fracture toughness and compressive strength. Cyclic oxidation tests were performed for 400 hours at the temperatures of 800 and 1000 °C. The cyclic oxidation tests simulate industrial processes, where the material is alternately exposed to elevated temperature and subsequent cooling (eg, engine components). From the viewpoint of most of the tested properties, alloying by niobium seems to be the most promising.
Order of Authors (with Contributor Roles):	Anna Knaislová, Dr.
	Vendula Šimůnková, Ing.
	Pavel Novák, assoc. prof.
	Filip Průša, Dr.
	Marcello Cabibbo, assoc. prof.
	Lucyna Jaworska, prof.
	Dalibor Vojtěch, prof.

Powered by Editorial Manager® and ProduXion Manager® from Aries Systems Corporation

Department of Metals and Corrosion Engineering
UCT PRAGUE

Prague, 19 November 2020

Dear Editor,

Please, find enclosed the electronic version of a manuscript of A. Knaislova, et al. “Effect of alloying elements on the properties of Ti-Al-Si alloys prepared by powder metallurgy”. This article is about preparation of innovative materials by using a various techniques of powder metallurgy, such as mechanical alloying, and Spark Plasma Sintering. Powder metallurgy has a good potential to substitute conventional melting metallurgy for these alloys in the future. The aim of this work is to investigated the effect of alloying elements and describe the properties of TiAl15Si15X15 alloy (X = Co, Cr, Fe, Mo, Nb, Ni)

This article follows up to previous articles of A. Knaislova, et al. “Combination of reaction synthesis and Spark Plasma Sintering in production of Ti-Al-Si alloys” and A. Knaislová, et al. “High-temperature oxidation of Ti-Al-Si alloys prepared by powder metallurgy” published in Journal of Alloys and Compounds. This article deepens knowledge about Ti-Al-Si alloys and describes improvement their properties using addition of other alloying elements, which is very important for possible further use in automobile or aerospace industry. We would like to ask you to consider this paper for publishing also in Journal of Alloys and Compounds.

Yours sincerely

Anna Knaislova
Department of Metals and Corrosion Engineering, UCT Prague
Czech Republic

Phone.: +420220444055, fax: +420220444400, e-mail: knaisloa@vscht.cz, www.vscht.cz

University of Chemistry and Technology, Prague, public university established by Act No. 111/1998 Coll., in the wording of subsequent regulations, based at Technická 5, 166 28 Prague 6 - Dejvice, Czech Republic, IČ: 60461373, DIČ: CZ-60461373,

The aim of the article was to find a way to improve the properties of Ti-Al-Si alloys prepared in our previous works. One of the possibilities was to test the addition of other alloying elements and characterization the effect of these elements on the microstructure, mechanical, tribological and high-temperature properties of Ti-Al-Si alloys prepared by mechanical alloying and Spark Plasma Sintering. In this work, the addition of cobalt, chromium, iron, molybdenum, niobium and nickel was tested.

Reviewer #2

1) The sentence "Molybdenum and niobium increase high-temperature and mechanical properties and niobium also fracture toughness [22, 23, 26]" has no clear meaning. I should be corrected.

The sentence was corrected.

2) Compression tests - the size of compression specimens and initial strain rate applied for compression testing are missing. How many compression specimens were tested for each alloy? It is necessary to add this information.

The information was added.

3) Dimensions of SPS tablets are missing. This information is very important for the readers.

The information was added.

4) Only compression tests were carried out for the alloys. How it is possible to report the ultimate tensile strength in Table 1? It is a major weakness, which cannot appear in the revised version of the manuscript. Table 1 and the relevant text need to be corrected.

The ultimate tensile strength is a mistake. The right term is ultimate compression strength. It was corrected.

5) Figs. 9, 10, 12 and 13 - it is very difficult to distinguish different alloys when these figures are printed in black and white. It should be better to use also different symbols not only different lines. The improvement is required.

All Figures were improved.

Reviewer #3

1) The only thing that should be checked is the quality of Figure 4 (since the small numbers in EDX data were not well readable due to poor quality), but maybe this is a problem of submission system.

The quality of Figure 4 was improved.

Manuscript Click here to access/download;Manuscript;Manuscript.docx

Effect of alloying elements on the properties of Ti-Al-Si alloys prepared by powder metallurgy

Anna Knaislová[1*], Vendula Šimůnková[1], Pavel Novák[1], Filip Průša[1], Marcello Cabibbo[2], Lucyna Jaworska[3], Dalibor Vojtěch[1]

[1]Department of Metals and Corrosion Engineering, University of Chemistry and Technology, Prague. Technická 5, 166 28 Prague, Czech Republic.

[2]DIISM/Università Politecnica delle Marche, Via Brecce Bianche 12, 60131 Ancona, Italy.

[3]Department of Materials Science and Non-Ferrous Metals Engineering, AGH University of Science and Technology, al. Mickiewicza 30, 30-059 Krakow, Poland

*corresponding author, E-mail: knaisloa@vscht.cz

Abstract

Intermetallic alloys based on Ti-Al-Si system are significant for their excellent high-temperature properties, especially for resistance against oxidation and achieving good mechanical properties at elevated temperatures. The main problem of these materials is high brittleness at room temperature, which could be solved by modifying the structure through the addition of other elements. In the previous work, selected alloying elements were added into the Ti-Al-Si alloys prepared by reactive sintering, but the properties did not meet the requirements for subsequent use in the automotive or aerospace industry, the materials had a very porous microstructure. Here, the addition of cobalt, chromium, iron, molybdenum, niobium and nickel into the TiAl15Si15 alloy prepared by mechanical alloying and Spark Plasma Sintering is tested and it is expected to improve the mechanical and high-temperature properties, in particular, fracture toughness. In this paper, the Ti-Al-Si alloys have been assessed on basis of microstructure, phase composition, mechanical and tribological properties, such as hardness, fracture toughness and strength in compression. Cyclic oxidation tests were performed for 400 hours at the temperatures of 800 and 1000 °C. The cyclic oxidation tests simulate industrial processes, where the material is alternately exposed to elevated temperature and subsequent cooling (eg, engine components). From the viewpoint of most of the tested properties, alloying by niobium seems to be the most promising.

Keywords: intermetallics, mechanical alloying, sintering, microstructure, mechanical properties, oxidation

1. Introduction

Ti-Al-Si alloys consist of titanium aluminides and titanium silicides. Aluminide phases are tougher than silicide phases. On the other hand, silicides are very hard but brittle phases. Ti-Al-Si alloys combine the properties of both phases and excel especially in low density, high-temperature oxidation and creep resistance [1-3]. The Ti_5Si_3 phase acts as a reinforcement for titanium aluminide matrix due to strength, it is also very good chemically, and mechanically compatible with TiAl (they have similar thermal expansion coefficients) [4].

The previous studies have shown that aluminium and silicon in Ti-Al-Si alloys reduce the oxidation rate of titanium to approximately 850 °C. Resistance against high-temperature oxidation is caused by the formation of protective layers of TiO_2 (rutile), Al_2O_3 (corundum) and SiO_2 (silica). In particular, the addition of silicon has a significant reduction effect on the oxidation rate due to the slow rate of oxygen diffusion in the SiO_2 layer in comparison with the diffusion rate in rutile (TiO_2) [5, 6]. Silicon also supports the formation of TiN (titanium nitride) between the base material and the oxide layer, where it forms a separate layer or insulated particles reinforcing the base material. Silicon reduces the solubility and diffusion rate of nitrogen in the titanium, and thus the titanium nitride is not formed in the Ti-Al alloy [5, 7-9].

One of the main factors limiting the wider use of Ti-Al-Si alloys is their low fracture toughness at room temperatures due to the missing area of plastic deformation at the tensile curve [10]. However, the plasticity of Ti-Al-Si alloys increases with the increasing temperature (DBTT) and can be improved by the addition of alloying elements. The limiting temperature of their use is set to 800 °C [11].

The addition of alloying elements (cobalt, chromium, iron, molybdenum, niobium and nickel) can improve strength, ductility and resistance to high-temperature oxidation of Ti-Al-Si alloys. There are few comprehensive studies on the effect of alloying elements on this alloy system [2, 12, 13]. The addition of cobalt improves the high-temperature properties and hardness of these materials [14, 15], chromium improves ductility, strength and oxidation resistance and creep [16]. Iron atoms primarily substitute aluminium positions in TiAl, so they cause substitution strengthening [17]. Molybdenum and niobium increase high-temperature and mechanical properties and niobium also fracture toughness [14, 15, 18]. Niobium also increases the thermodynamic activity of aluminium compared to titanium and thus supports the

formation of a stable Al_2O_3 layer. It also supports the formation of TiN layer at the interface between the oxide layer and the base material [19]. Nickel improves high-temperature properties [20].

The aim of this work is to describe the properties of TiAl15Si15X15 alloy (X = Co, Cr, Fe, Mo, Nb, Ni) prepared by mechanical alloying followed by Spark Plasma Sintering method. In this paper, microstructure, phase composition, selected mechanical and tribological properties and high-temperature oxidation are shown and the properties are compared with the ternary TiAl15Si15 alloy.

2. Material and methods

2.1. Preparation of intermediary phases by mechanical alloying and consolidation by Spark Plasma Sintering

Powders of intermetallic alloys TiAl15Si15X15 (wt. %), where X = Co, Cr, Fe, Mo, Nb, Ni, were prepared by powder metallurgy method using mechanical alloying. Pure powders were used as starting materials: titanium (purity 99.5 %, particle size < 50 μm), aluminium (purity 99.7 %, particle size < 50 μm), silicon (purity 99.5 %, particle size < 50 μm), cobalt (purity 99.8 %, particle size 2 μm), chromium (purity 99 %, particle size < 150 μm), iron (purity 99.9 %, particle size < 150 μm), molybdenum (purity 99 %, particle size < 150 μm), niobium (purity 99 %, particle size < 150 μm) and nickel (purity 99.99 %, particle size < 150 μm) powder. The prepared powder mixtures weighing 5 grams were placed in a milling vessel and mechanically alloyed in a planetary ball mill Retsch PM 100. Metal powders were ground with 10 milling balls (ball to powder ratio of approximately 60:1). The milling vessel was filled with an inert gas (argon) to prevent the oxidation of powders. The parameters of mechanical alloying were chosen based on our previous research [4], the powders were milled 4 hours with 400 rpm and after 30 minutes the direction of rotation was changed.

Thus prepared powders were compacted by SPS (Spark Plasma Sintering). The sintering process was carried out at a temperature of 1100 °C for 15 minutes, a pressure of 80 MPa, in a continuous current flow mode and the resulting tablets were cooled continuously with a rate of 50 °C/min.

2.2. Phase composition and microstructure of TiAl15Si15X15 alloys

The phase composition of milled powders, as well as compacted alloys, was examined by X-ray diffraction analysis by the means of a diffractometer PANalytical XPert Pro, diffraction patterns were evaluated in PANalytical HighScore plus program using the PDF2 database. The metallographic samples were prepared using grinding papers P80 to P4000, the ground samples were then polished with a polishing suspension Eposil F (a mixture of silica particles with hydrogen peroxide). The samples thus prepared were etched with modified Kroll´s reagent (10 ml HF, 5 ml HNO_3 and 85 ml H_2O). The microstructure was observed using an optical light microscope Olympus PME3 with Carl Zeiss AxioCam ICc3 digital camera and AxioVision program. The detailed microstructure and the composition of individual phases of the samples was investigated by scanning electron microscope TESCAN VEGA 3 LMU equipped with energy

dispersive analyser (SEM-EDS). The porosity and pore size were determined by microstructure images of non-etched compact alloys and evaluated by program Lucia 4.8.

2.3. Mechanical tests of TiAl15Si15X15 alloys

Mechanical properties were tested on the compacted alloys. Compressive strength tests were performed on a LabTest testing machine 5.250SP1-VM. Hardness and microhardness were measured using Vickers hardness with a load of 1 kg (HV 1) and 0.1 kg (HV 0.1) on the Future-Tech FM-700 machine. Fracture toughness was evaluated based on the crack size on the image analysis and determined by calculation according to Palmqvist equation (1):

$$K_c = 0.016 \cdot \left(\frac{E}{HV}\right)^{\frac{1}{2}} \cdot \left(\frac{F}{c^{\frac{3}{2}}}\right) \quad (1)$$

where Kc is fracture toughness ($MPa \cdot m^{1/2}$), E is the modulus of elasticity (GPa), HV is the Vickers hardness (HV 1, GPa), F is the load (N) and c is a half of crack length (mm). Abrasive wear resistance was carried out by a modified pin-on-disc method on a disc tribometer. Each tested sample passed approximately 2.5 km distance in 15 minutes on P1200 grinding paper with 5.8 N normal force. The resulting wear rate was calculated based on equation (2):

$$w = \frac{\Delta m}{\rho \cdot l} \quad (2)$$

where w is the wear rate ($cm^3 \cdot m^{-1}$), Δm is the mass loss (g), l denotes the path length on grinding paper (m) ρ is a density of sample ($g \cdot cm^{-3}$). The density was measured by the Archimedes method.

2.4. High-temperature oxidation tests of TiAl15Si15X15 alloys

Cyclic oxidation tests are intended to help simulate industrial processes where the material is exposed to elevated temperatures and subsequent cooling. The temperature of 800 °C was chosen according to the temperature of the applicability of Ti-Al alloys. The temperature of 1000 °C was chosen for the examination of the possibility of increasing the thermal stability by the addition of silicon. The alloy samples were annealed for 400 hours. The samples are removed from the furnace after 50-hours intervals, air-cooled, weighed and then returned to the furnace to the given temperature.. The internal stress occurs between the base metal and its oxide layer as the consequence of cyclically repeated annealing. The sample and the sample with scaled-off oxides were weighed after every 50 hours. The oxide layer was observed using an

optical and scanning electron microscope. The thickness of the oxide layer was measured by image analysis using ImageJ program. The values of parabolic constants were calculated according to equation (3):

$$K_p = \frac{\left(\frac{\Delta m}{A}\right)^2}{t} \quad (3)$$

where K_p is the parabolic constant ($g^2 \cdot m^4 \cdot h^{-1}$), Δm is the weight gain (g), A is the sample area (m^2) and t is the duration of cyclic oxidation (h).

3. Results

The addition of alloying elements to Ti-Al-Si alloys was tested to improve the properties of the material. Ti-Al-Si-X alloys were prepared by a combination of mechanical alloying and Spark Plasma Sintering (MA+SPS) to maintain a fine-grained structure. Cobalt, chromium, iron, molybdenum, niobium and nickel were selected from the alloying elements. Cobalt improves high-temperature properties and hardness, chromium ductility, strength and oxidation resistance, iron strength, molybdenum with niobium high-temperature and mechanical properties, niobium should increase fracture toughness and nickel high-temperature properties.

3.1. Phase composition and microstructure of TiAl15Si15X15 powders

The optimal duration of mechanical alloying (MA) of TiAl15Si15X15 (X = Co, Cr, Fe, Mo, Nb, Ni) powders was chosen on the basis of the previous research [4]. After 4 hours of MA, all pure element powders have reacted and formed intermetallic phases. The phase composition of the mechanically alloyed powders is described by X-ray diffractograms in Figure 1. All alloys are formed by Ti_5Si_3 and TiAl stable phases. A metastable phase $Al_{80}Cr_{20}$ in TiAl15Si15Cr15 alloy is also formed. Furthermore, it can be assumed that all phases are substituted by other elements, as shown by the shift of the diffraction lines in the XRD pattern. The alloying elements do not form separate phases but dissolve in titanium silicide or titanium aluminide.

The microstructure of TiAl15Si15X15 powders prepared by MA is shown in Fig. 2. Micrographs show that the powder particles have a homogeneous structure. Regions of different compositions are not visible, except for areas with higher amount of iron. All mechanically alloyed powders were contaminated by iron from the material of the milling vessel - light areas in the figures. The particle size of alloy powder after MA varies in the order of tens of micrometers. Titanium with silicon form Ti_5Si_3 titanium silicides, titanium with

aluminium form TiAl titanium aluminide. Numerous cracks in the microstructure suggest the formation of brittle intermetallic phases.

3.2. Phase composition and microstructure of TiAl15Si15X15 compact alloys

Figure 3 shows the phase composition of TiAl15Si15X15 alloys prepared by mechanical alloying (MA) and Spark Plasma Sintering (SPS) using X-ray diffraction. All alloys are formed by Ti_5Si_3 titanium silicide, which is preferably formed because silicon has a high affinity to titanium. Silicides of alloying elements (cobalt, chromium, iron, niobium and nickel) are also present in the structure. The silicides are generally very hard and brittle phases. Titanium aluminides TiAl are also present in the alloy structure and they are tougher than silicides. Aluminides of other alloying elements were not identified as separate phases, although these elements (Co, Fe, Nb, Ni) form stable aluminides. It can be assumed that phases of unbalanced composition (i.e mixed aluminides and silicides), which are supersaturated to the equilibrium composition, are present in the structure of Ti-Al-Si-X alloys prepared by MA and SPS.

Figure 4 shows the microstructure of TiAl15Si15X15 (X = Co, Cr, Fe, Mo, Nb, Ni) alloys prepared by mechanical alloying followed by Spark Plasma Sintering. The microstructure is very fine-grained, well sintered and without the presence of unreacted basic elements. The structure of alloys consists of titanium silicides, selected silicides of alloying elements and titanium aluminide TiAl. Using the EDS point analysis elemental composition of various regions of microstructure was found. It cannot completely distinguish areas rich in individual phases. Lighter areas indicate the presence of heavier elements such as iron or silicon. Darker areas appear to be richer in aluminium. Numerous cracks were also detected in the microstructure of alloys, which are likely to arise due to anisotropy of the thermal expansion coefficient of Ti_5Si_3 phase in different crystal directions [1]. Iron contamination from the grinding vessel was found in all alloys.

The porosity of TiAl15Si15X15 alloys does not exceed 3 vol. % (Fig. 5). Alloy with nickel reaches the highest porosity. The remaining alloys reach the porosity under 1 vol. %. Average equivalent diameter of pores is from 4.5 to 7 μm (Fig. 5).

3.3. Mechanical and tribological tests of TiAl15Si15X15 compact alloys

All mechanical and tribological tests were measured on compact samples. The hardness of all Ti-Al-Si-X alloys exceeds 1000 HV 1 (Fig. 6). Alloy with iron reaches the highest hardness (1330 HV 1), followed by alloy with cobalt and nickel. The alloy containing molybdenum has the lowest hardness (1026 HV 1).

The values of microhardness (HV 0.1) exceed 1500 HV 0.1 and range from 1527 HV 0.1 in the case of TiAl15Si15Co15 alloy up to 1813 HV 0.1 for TiAl15Si15Mo15 alloy (Fig. 7). The high values of microhardness of all alloys indicate significant reinforcement by alloying elements. The highest values of microhardness were achieved by alloy with molybdenum and niobium. These elements are able to substitute titanium position in titanium aluminide (TiAl) and thus strengthen it significantly. The microhardness value HV 0.1 of the TiAl15Si15Co15 alloy is the lowest of all alloys and the hardness value HV 1 is the second-highest for this alloy, proving the sensitivity of this method to phase distribution.

Fracture toughness of all alloys is low, i.e. all alloys tend to brittle fracture (Fig. 8). The highest value of fracture toughness was reached by alloy with chromium (1.7 $MPa \cdot m^{1/2}$), the addition of chromium has a significant effect on the increase of toughness of titanium aluminides [14]. On the other hand, alloy with cobalt achieved the lowest value (0.69 $MPa \cdot m^{1/2}$) due to a higher portion of silicides, cracks and especially pores in the microstructure, which behave as material imperfections. A stress concentration occurs at the edges of the microcrack. Then a certain stress value is reached, which leads to disruption of the bonds between atoms to form new surfaces [21].

The compression tests of Ti-Al-Si-X alloys were carried out at room temperature and the tests ended by fracture of material (Fig. 9). The absence of yield strength on compression curves indicates a missing area of plastic deformation, the mechanically alloyed Ti-Al-Si-X alloys are brittle. The values of ultimate tensile strength vary for each alloy, mainly because of the occurrence of cracks and pores in the microstructure of alloys. The highest ultimate tensile strength was reached by TiAl15Si15Mo15 alloy (2298 MPa). Alloys containing niobium and iron exceeded the limit of 2000 MPa in at least one of the performed tests. The lowest ultimate tensile strength was reached by TiAl15Si15Co15 alloy due to the large number of structural inhomogenities.

Ti-Al-Si-X alloys achieve very good values of abrasive wear resistance (Fig. 10). The wear rate of all alloys is very low, the lowest values were achieved by alloy with molybdenum, niobium and iron. The high abrasive wear resistance corresponds to the high ultimate tensile strength and hardness of these alloys.

3.4. High-temperature oxidation tests of TiAl15Si15X15 compact alloys

Fig. 11 shows the time dependence of the weight gain of Ti-Al-Si-X alloys during cyclic oxidation at 800 °C. It can be shown from the graph that the highest weight gain was found for alloys with cobalt and

iron and in one case also for alloys with molybdenum, but the values are minimal and comparable with tests of Ti-Al-Si alloys without alloying elements also prepared by MA+SPS [2]. On the contrary, an almost negligible weight gain was found in alloys with chromium and niobium, which confirmed the very positive effect of these elements on high-temperature properties. The oxidation kinetics is probably controlled by a chemical reaction (linear course of the curve) for alloys with cobalt and iron, for others, it is a diffusion control (parabolic dependence). Fig. 12 shows the number of scaled-off oxides formed during cyclic oxidation at 800 °C. It can be seen from the graph that the amount of delaminated oxides is almost negligible for all alloys (the change in weight is in thousands of grams), which means that all oxide layers are cohesive and there is no peeling of oxides (which can be confirmed in Fig. 13, where the compact surface of each alloy is visible).

Fig. 14 shows the time dependence of the weight gain of Ti-Al-Si-X alloys during cyclic oxidation at 1000 °C. In the figure, it is possible to see the parabolic growth of the oxide layer in the case of an alloy with molybdenum, chromium and niobium. In the sample of alloys with nickel, cobalt and iron, there was a weight loss of the sample, which indicates the formation of no-adherent oxide layer, which delaminated during the oxidation test, as confirmed by Figures 15 and 16. The cobalt-alloyed alloy broke after 400 hours of oxidation (Fig. 16).

The phase composition of the oxide layer of Ti-Al-Si-X alloys was determined by X-ray diffraction analysis and the results are shown in tab. 1. The oxide layer consists of titanium dioxide (rutile), alumina (corundum) and silica. The oxide layer is also formed by oxides of alloying elements (MoO_2, MoO_3, Fe_2O_3) and mixed oxides (Al_2TiO_5, $FeTiO_3$). In addition to oxygen, nitrogen also penetrates from the air into the alloy, forming nitrides found in the alloy with iron (Fe_3N) and niobium (AlN, Nb_2N). In the alloy with molybdenum, niobium and nickel, aluminide and titanium silicide, which belong to the base material, were also detected in the oxide layer. These phases were found by X-ray diffraction because the oxide layer after oxidation at 800 °C is very thin and also a crack could be found at the diffraction site.

Table 1 Phase composition of the surface oxide layer of Ti-Al-Si-X alloys after 400 hours of cyclic oxidation

Alloy	**Phase composition (cyclic oxidation, 800 °C)**	**Phase composition (cyclic oxidation, 1000 °C)**

TiAl15Si15Co15	TiO_2, Al_2O_3, SiO_2	TiO_2, Al_2O_3, SiO_2
TiAl15Si15Cr15	TiO_2, Al_2O_3, SiO_2, Al_2TiO_5	TiO_2, Al_2O_3, SiO_2
TiAl15Si15Fe15	TiO_2, Al_2O_3, SiO_2, Fe_2O_3	TiO_2, Al_2O_3, SiO_2, Fe_3N, $FeTiO_3$
TiAl15Si15Mo15	TiO_2, Al_2O_3, MoO_3, Ti_5Si_3	TiO_2, SiO_2, MoO_2
TiAl15Si15Nb15	TiO_2, Al_2O_3, SiO_2, AlN, Ti_5Si_3	TiO_2, Al_2O_3, SiO_2, AlN, Nb_2N
TiAl15Si15Ni15	TiO_2, Al_2O_3, SiO_2, $TiAl_3$	TiO_2, Al_2O_3, SiO_2

The following Fig. 17 and Fig. 18 shows the microstructure of the oxide layers of TiAl15Si15X15 alloys, the figure on the left always shows the appearance of the layer after oxidation at 800 °C, on the right after oxidation at 1000 °C. It can be seen from the figures that after oxidation at 800 °C, the alloy with cobalt, iron and nickel formed the thickest oxide layer, which was approximately 40 μm thick, while the alloy with chromium or niobium formed almost no observable oxide layer on the surface. For oxidation at 1000 °C, the results were similar, the least resistant was again the alloy with cobalt, iron and nickel and the most resistant was the alloy with chromium and niobium. The images show that some oxide layers are cracked. Cracks most often appear at the base material-oxide layer interface.

The elemental composition of individual parts of the oxide layer was determined by EDS analysis. The outer part of the oxide layer is made of titanium dioxide, under which there are silica and alumina. In the inner part of the oxide layer, there is a higher proportion of alloying elements and we can also find selected oxides of iron or molybdenum. Using EDS analysis, no nitrogen-rich areas were found in any alloy.

4. Discussion

TiAl15Si15X15 alloys are all formed by the stable titanium silicide Ti_5Si_3 and silicides of the alloying elements (cobalt, chromium, iron, niobium and nickel). The aluminide matrix in all alloys is the TiAl phase, which is also found in the TiAl15Si15 alloy [4]. In articles [15, 22], TiAl15Si15X15 alloys were prepared by reactive sintering. The article described that some of the used alloying elements are mainly aluminide-forming (cobalt, copper and nickel), others silicide-forming (iron) and chromium with molybdenum form stable aluminides and silicides. SEM-EDS analysis showed that TiAl15Si15X15 alloys prepared by reactive sintering do not form detectable amounts of silicides and aluminides of added alloying elements and only mixed silicides/aluminides are formed, where the alloying elements dissolve in titanium silicides and

aluminides [2, 15]. TiAl15Si15X15 alloys in this work were prepared by mechanical alloying, where X-ray analysis of the powders did not show the formation of silicides or aluminides of the alloying elements after MA. After Spark Plasma Sintering, the formation of silicides of alloying elements (cobalt silicide CoSi, chromium silicide CrSi, iron silicide Fe_2Si, niobium silicide Nb_5Si_3 and nickel silicide Ni_2Si) was confirmed by X-ray diffraction. None of these silicides were found in samples prepared by reactive sintering. In the TiAl15Si15Fe15 alloy, a mixture of titanium aluminides TiAl and Ti_3Al was found after reactive sintering, while after MA+SPS only titanium aluminide TiAl was found. The results of the EDS analysis showed that the alloying elements do not form a detectable amount of their own phases during reactive sintering, they only dissolve in titanium silicides or aluminides. After SPS, the silicides of the alloying elements arise.

Mechanical alloying causes aluminium in titanium aluminides to be strongly substituted with silicon and vice versa in titanium silicides. The authors described that Ti(Al,Si) supersaturated solid solutions are formed after at least 10 to 20 hours of milling [23, 24], but as shown in this work, intermetallic phases are formed during a much shorter mechanical alloying duration (after 4 hours). Mechanical alloying in combination with Spark Plasma Sintering leads to a very fine microstructure of the investigated alloys. The authors described that mechanical alloying is a very efficient process for obtaining nanometer-sized grains [25, 26]. The refinement of Ti_5Si_3 crystallites is probably due to strong deformation and subsequent recrystallization. The distribution of titanium silicides is much more homogeneous because the brittle powder is crushed into very fine particles during the first step of the mechanical alloying. The elements in the obtained compounds are substituted for each other, which exceeds the limits of equilibrium solubility [27]. Fine-grained microstructure due to mechanical alloying and higher compaction pressure significantly reduced the porosity of alloys compared to alloys prepared by reactive sintering [15]. The porosity of the TiAl15Si15 alloy prepared by MA+SPS was 0.4 % by volume [4]. The addition of chromium and molybdenum slightly increased the porosity (to 0.7 % by volume and 0.8 % by volume, respectively), the addition of iron tripled the value (to 1.2 % by volume) and the addition of cobalt even increased fivefold (to 2 % by volume). The same effect of these alloying elements is also mentioned in articles [15, 22]. The article [15] further shows that the addition of nickel reduces the porosity, however, the opposite effect was found in this work. The TiAl15Si15Ni15 alloy had the same high porosity value as the alloy with cobalt. Only

niobium as an alloying element did not increase the porosity, the TiAl15Si15Nb15 alloy had the same porosity as the TiAl15Si15 alloy without alloying elements.

The microhardness values of all TiAl15Si15X15 alloys are higher than the values for the TiAl15Si15 alloy prepared by MA+SPS [28] because the alloys were further strengthened by the addition of alloying elements. Also, the increase in hardness may be associated with the strengthening of hard particles of titanium silicides by alloying elements [15]. Molybdenum and niobium replace the positions of titanium in titanium aluminide TiAl, thus significantly strengthening it, so the microhardness of these alloys was the highest of all tested. Along with the hardness, the alloying elements also increased the ultimate tensile strength values, except for the alloy with cobalt or nickel, where there were numerous cracks in the microstructure. The article [22] shows that all alloying elements added to Ti-Al-Si alloys prepared by reactive sintering decrease mechanical properties, especially fracture toughness. In our case, however, the fracture toughness did not decrease, on the contrary, the fracture toughness reached higher values compared to TiAl15Si15 alloy without alloying elements [28]. The TiAl15Si15Cr15 alloy prepared by ML + SPS reached the best values of fracture toughness of all tested alloys.

The high-temperature oxidation can be controlled by diffusion or chemical reactions. If the growth of the oxide layer proceeds through a diffusion-controlled mechanism, the resulting growth of the oxide layer to the annealing time has a parabolic dependence. During the oxidation, the oxide layer grows to a certain limit, where the diffusion of oxygen into the material is limited. The layer on the material no longer grows, so it protects the material well. The linear dependence of the kinetic curve is associated with the formation of an oxide layer by chemical reaction-controlled process. This mechanism applies primarily when the material has a porous oxide layer or contains a significant amount of cracks, and so oxygen from the surrounding atmosphere can easily penetrate into the depth of the material. Likewise, this mechanism applies to the destroying of the oxide layer (pores, cracks). The formation of the oxide layer can be determined based on values of parabolic constant Kp. If the value of the parabolic constant does not change over time, it indicates the diffusion-controlled mechanism. The high-temperature behaviour of Ti-Al-Si alloys was detailed described in our previous articles [2, 11, 29, 30].

The authors described that the high-temperature behaviour of Ti-Al-Si alloys can be improved by the addition of other alloying elements. The addition of niobium was the most studied [31-36]. The combination

of silicon and niobium resulted in much better oxidation resistance than with the addition of individual elements. Cobalt, chromium, copper, iron, molybdenum and nickel also increase the resistance to oxidation at 1000 °C [15]. In this article [15] the Ti-Al-Si-based alloy prepared by reactive sintering and containing 15 wt. % molybdenum had the best oxidation resistance, followed by an alloy with chromium. These two alloys also showed very good thermal stability [15, 22]. The positive influence of alloying elements for the oxidation resistance of Ti-Al-Si alloys was also confirmed in this work. All alloys had very good adhesion of the oxide layer, which was relatively thin, and the minimum scaled-off oxides occurred only at a temperature of 1000 °C. The most oxidation-resistant samples were alloyed with chromium and niobium, which confirms the positive effect of these elements on oxidation resistance.

5. Conclusions

Ti-Al-Si alloys prepared by mechanical alloying have a homogeneous and fine-grained microstructure with low porosity, which ensures high mechanical properties. Ti-Al-Si alloys are extremely resistant at temperatures up to 800 °C. The addition of alloying elements improved the properties of Ti-Al-Si alloys. Along with hardness, the alloying elements also increased the compressive strength values. The TiAl15Si15Cr15 alloy achieved the best values of fracture toughness of all tested alloys. The best oxidation resistance was achieved by an alloy with niobium and chromium.

Acknowledgement

This work was supported from the grant of Specific university research – grant No A1_FCHT_2020_003 and A2_FCHT_2020_046.

References

[1] N.S. Stoloff, V.K. Sikka, Physical metallurgy and processing of intermetallic compounds, Chapman & Hall, 1996.

[2] A. Knaislová, P. Novák, F. Průša, M. Cabibbo, L. Jaworska, D. Vojtěch, High-temperature oxidation of Ti–Al–Si alloys prepared by powder metallurgy, Journal of Alloys and Compounds, 810 (2019) 151895.

[3] A. Lasalmonie, Intermetallics: Why is it so difficult to introduce them in gas turbine engines?, Intermetallics, 14 (2006) 1123-1129.

[4] A. Knaislová, J. Linhart, P. Novák, F. Průša, J. Kopeček, F. Laufek, D. Vojtěch, Preparation of TiAl15Si15 intermetallic alloy by mechanical alloying and the spark plasma sintering method, Powder Metallurgy, 62 (2019) 56-60.

[5] P. Novák, Příprava, vlastnosti a použití intermetalických sloučenin, Chemické listy, 106 (2012) 884-889.

[6] N.S. Stoloff, C.T. Liu, S.C. Deevi, Emerging applications of intermetallics, Intermetallics, 8 (2000) 1313-1320.

[7] R. Nesper, Intermetallics. Von G. Sauthoff. VCH Verlagsgesellschaft, Weinheim, 1995. 165 S., geb. 128.00 DM. – ISBN 3-527-29320-5, Angewandte Chemie, 108 (1996) 726-727.

[8] D. Shi, B. Wen, R. Melnik, S. Yao, T. Li, First-principles studies of Al–Ni intermetallic compounds, Journal of Solid State Chemistry, 182 (2009) 2664-2669.

[9] C.L. Yeh, H.J. Wang, W.H. Chen, A comparative study on combustion synthesis of Ti–Si compounds, Journal of Alloys and Compounds, 450 (2008) 200-207.

[10] A. Knaislová, P. Novák, M. Cabibbo, F. Průša, C. Paoletti, L. Jaworska, D. Vojtěch, Combination of reaction synthesis and Spark Plasma Sintering in production of Ti-Al-Si alloys, Journal of Alloys and Compounds, 752 (2018) 317-326.

[11] A. Knaislová, V. Šimůnková, P. Novák, F. Průša, High-temperature behaviour of Ti-Al-Si alloys prepared by Spark Plasma Sintering, Manufacturing Technology, 17 (2017) 733-738.

[12] P. Novák, F. Průša, J. Šerák, D. Vojtěch, A. Michalcová, Oxidation resistance and thermal stability of Ti-Al-Si alloys produced by reactive sintering, Metal, (2009).

[13] X. Lu, X.B. He, B. Zhang, X.H. Qu, L. Zhang, Z.X. Guo, J.J. Tian, High-temperature oxidation behavior of TiAl-based alloys fabricated by spark plasma sintering, Journal of Alloys and Compounds, 478 (2009) 220-225.

[14] G. Sauthoff, Intermetallics, VCH, Weinheim, New York, Basel, Cambridge, Tokyo, 1995.

[15] P. Novák, J. Kříž, F. Průša, J. Kubásek, I. Marek, A. Michalcová, M. Voděrová, D. Vojtěch, Structure and properties of Ti–Al–Si-X alloys produced by SHS method, Intermetallics, 39 (2013) 11-19.

[16] M.P. Brady, J.L. Smialek, D.L. Humphrey, J. Smith, The role of Cr in promoting protective alumina scale formation by γ-based Ti-Al-Cr alloys— II. Oxidation behavior in air, Acta Materialia, 45 (1997) 2371-2382.

[17] G. Ghosh, Al-Fe-Ti (Aluminium - Iron - Titanium), in: G. Effenberg, S. Ilyenko (Eds.) Light Metal Systems. Part 2: Selected Systems from Al-Cu-Fe to Al-Fe-Ti, Springer Berlin Heidelberg, Berlin, Heidelberg, 2005, pp. 1-27.

[18] Y. Lu, J. Yamada, J. Nakamura, K. Yoshimi, H. Kato, Effect of B2-ordered phase on the deformation behavior of Ti-Mo-Al alloys at elevated temperature, Journal of Alloys and Compounds, 696 (2017) 130-135.

[19] H. Jiang, M. Hirohasi, Y. Lu, H. Imanari, Effect of Nb on the high temperature oxidation of Ti–(0–50 at.%)Al, Scripta Materialia, 46 (2002) 639-643.

[20] J. Shi, A. Zheng, Z. Lin, R. Chen, J. Zheng, Z. Cao, Effect of process control agent on alloying and mechanical behavior of L21 phase Ni–Ti–Al alloys, Materials Science and Engineering: A, 740-741 (2019) 130-136.

[21] J. Pluhař, Nauka o materiálech, SNTL, 1989.

[22] P. Novák, J. Kříž, A. Michalcová, D. Vojtěch, Effect of alloying elements on properties of PM Ti-Al-Si alloys, Acta Metallurgica Slovaca, 19 (2013) 240-246.

[23] K.P. Rao, J.B. Zhou, Characterization of mechanically alloyed Ti–Al–Si powder blends and their subsequent thermal stability, Materials Science and Engineering: A, 338 (2002) 282-298.

[24] A. Vyas, K.P. Rao, Y.V.R.K. Prasad, Mechanical alloying characteristics and thermal stability of Ti–Al–Si and Ti–Al–Si–C powders, Journal of Alloys and Compounds, 475 (2009) 252-260.

[25] G. Liang, Q. Meng, Z. Li, E. Wang, Consolidation of nanocrystalline Al-Ti alloy powders synthesized by mechanical alloying, Nanostructured Materials, 5 (1995) 673-678.

[26] H.A. Calderon, V. Garibay-Febles, M. Umemoto, M. Yamaguchi, Mechanical properties of nanocrystalline Ti–Al–X alloys, Materials Science and Engineering: A, 329-331 (2002) 196-205.

[27] P. Haušild, M. Karlík, J. Čech, F. Průša, K. Nová, P. Novák, P. Minárik, J. Kopeček, Preparation of Fe-Al-Si Intermetallic Compound by Mechanical Alloying and Spark Plasma Sintering, Acta Physica Polonica A, 134 (2018).

[28] A. Knaislová, P. Novák, J. Kopeček, F. Průša, Properties Comparison of Ti-Al-Si Alloys Produced by Various Metallurgy Methods, Materials, 12 (2019) 3084.

[29] A. Knaislová, V. Šimůnková, P. Novák, High-temperature oxidation of intermetallics based on Ti-Al-Si system, Manufacturing Technology, 18 (2018) 255-258.

[30] P. Novák, F. Průša, J. Šerák, D. Vojtěch, A. Michalcová, High-temperature behaviour of Ti–Al–Si alloys produced by reactive sintering, Journal of Alloys and Compounds, 504 (2010) 320-324.

[31] K. Maki, M. Shioda, M. Sayashi, T. Shimizu, S. Isobe, Effect of silicon and niobium on oxidation resistance of TiAl intermetallics, in: S.H. Whang, D.P. Pope, C.T. Liu (Eds.) High Temperature Aluminides and Intermetallics, Elsevier, Oxford, 1992, pp. 591-596.

[32] H.-r. Jiang, Z.-l. Wang, W.-s. Ma, X.-r. Feng, Z.-q. Dong, L. Zhang, Y. Liu, Effects of Nb and Si on high temperature oxidation of TiAl, Transactions of Nonferrous Metals Society of China, 18 (2008) 512-517.

[33] M. Terner, S. Biamino, G. Baudana, A. Penna, P. Fino, M. Pavese, D. Ugues, C. Badini, Initial Oxidation Behavior in Air of TiAl-2Nb and TiAl-8Nb Alloys Produced by Electron Beam Melting, Journal of Materials Engineering and Performance, 24 (2015) 3982-3988.

[34] D. Vojtěch, J. Čížkovský, P. Novák, J. Šerák, T. Fabián, Effect of niobium on the structure and high-temperature oxidation of TiAl–Ti5Si3 eutectic alloy, Intermetallics, 16 (2008) 896-903.

[35] D. Vojtěch, T. Popela, J. Kubásek, J. Maixner, P. Novák, Comparison of Nb- and Ta-effectiveness for improvement of the cyclic oxidation resistance of TiAl-based intermetallics, Intermetallics, 19 (2011) 493-501.

[36] J.S. Wu, L.T. Zhang, F. Wang, K. Jiang, G.H. Qiu, The individual effects of niobium and silicon on the oxidation behaviour of Ti3Al based alloys, Intermetallics, 8 (2000) 19-28.

Figure and table captions

Fig. 1 XRD patterns of TiAl15Si15X15 powders

Fig. 2 Scanning electron micrographs of TiAl15Si15X15 (X = Co, Cr, Fe, Mo, Nb, Ni) powders prepared by mechanical alloying

Fig. 3 XRD patterns of TiAl15Si15X15 compact alloys

Fig. 4 Scanning electron micrographs of TiAl15Si15X15 (X = Co, Cr, Fe, Mo, Nb, Ni) alloys prepared by mechanical alloying and Spark Plasma Sintering

Fig. 5 Porosity and pore size of TiAl15Si15X15 compact alloys

Fig. 6 Hardness of TiAl15Si15X15 compact alloys

Fig. 7 Microhardness of TiAl15Si15X15 compact alloys

Fig. 8 Fracture toughness of TiAl15Si15X15 compact alloys

Fig. 9 Compression tests of TiAl15Si15X15 compact alloys

Fig. 10 Abrasive wear resistance of TiAl15Si15X15 compact alloys

Fig. 11 Time dependence of the Ti–Al–Si-X alloys (MA+SPS) mass gain during cyclic oxidation at 800 °C

Fig. 12 Time dependence of the scaled-off oxides (MA+SPS) mass gain during cyclic oxidation at 800 °C

Fig. 13 Appearance of Ti–Al–Si-X alloys (MA+SPS) after 400 h of cyclic oxidation at 800 °C: a) TiAl15Si15Co15, b) TiAl15Si15Cr15, c) TiAl15Si15Fe15, d) TiAl15Si15Mo15, e) TiAl15Si15Nb15, f) TiAl15Si15Ni15

Fig. 14 Time dependence of the Ti–Al–Si-X alloys (MA+SPS) mass gain during cyclic oxidation at 1000 °C

Fig. 15 Time dependence of the scaled-off oxides (MA+SPS) mass gain during cyclic oxidation at 800 °C

Fig. 16 Appearance of Ti–Al–Si-X alloys (MA+SPS) after 400 h of cyclic oxidation at 1000 °C: a) TiAl15Si15Co15, b) TiAl15Si15Cr15, c) TiAl15Si15Fe15, d) TiAl15Si15Mo15, e) TiAl15Si15Nb15, f) TiAl15Si15Ni15

Fig. 17 Microstructure (SEM) of the Ti–Al–Si-X alloys (MA+SPS) after cyclic oxidation (400 h): a) TiAl15Si15Co15, b) TiAl15Si15Cr15, c) TiAl15Si15Fe15

Fig. 18 Microstructure (SEM) of the Ti–Al–Si-X alloys (MA+SPS) after cyclic oxidation (400 h): a) TiAl15Si15Mo15, b) TiAl15Si15Nb15, c) TiAl15Si15Ni15

Table 1 Phase composition of the surface oxide layer of Ti-Al-Si-X alloys after 400 hours of cyclic oxidation

- Ti-Al-Si-X (X=Co, Cr, Fe, Mo, Nb, Ni) alloys prepared using mechanical alloying and Spark Plasma Sintering
- Alloys have fine-grained and homogeneous microstructure with low porosity.
- Alloyed elements increased hardness and compressive strength values.

Figure 2

Click here to access/download;Figure;Fig. 2.tif

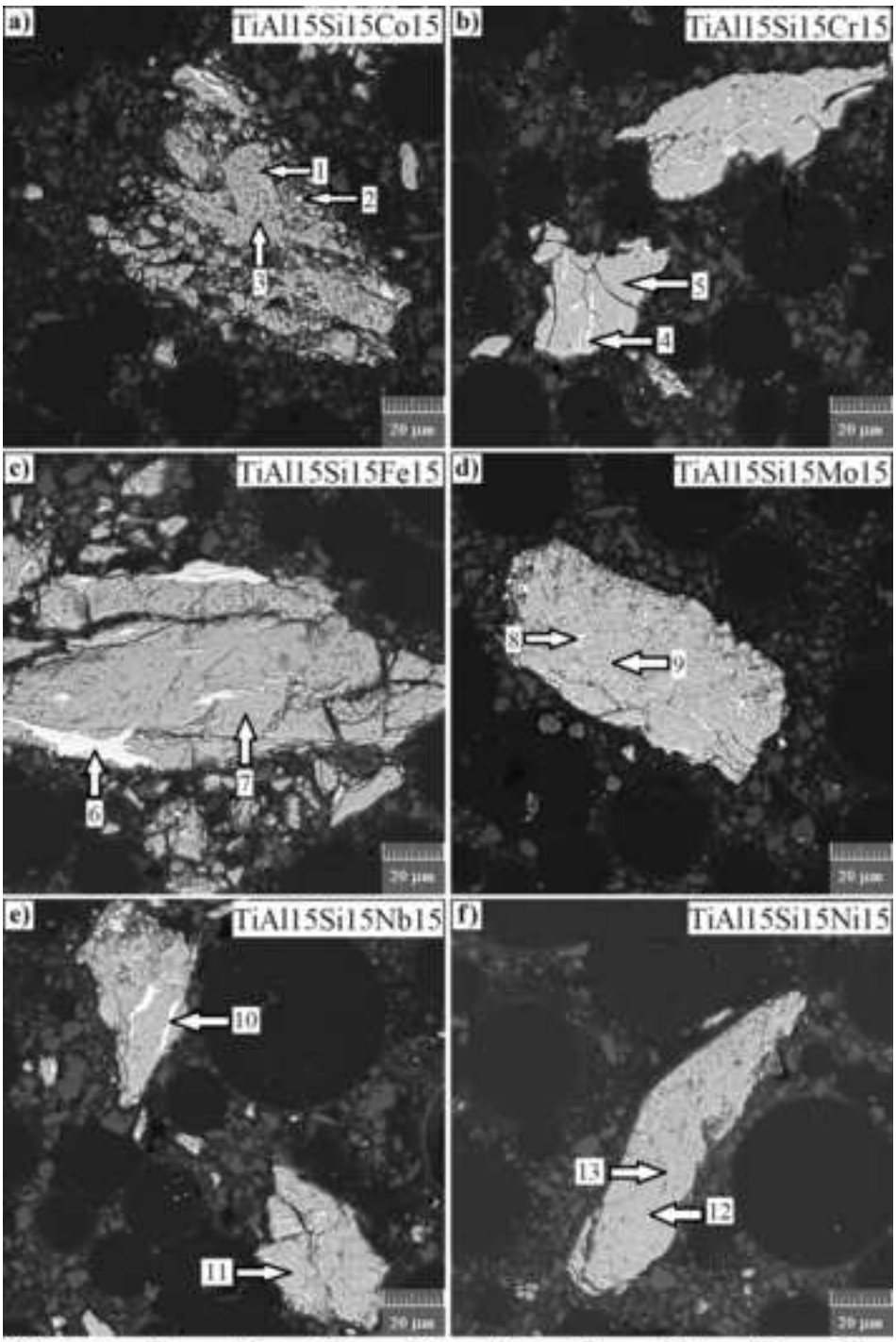

Spectrum	Ti	Al	Si	Co	Cr	Fe	Mo	Nb	Ni
1	46.9	21.3	24.6	7.3	-	-	-	-	-
2	9.9	6.5	8.4	6.7	9.8	65.5	-	-	-
3	49.6	21.5	19.4	9.4	-	-	-	-	-
4	16.6	12.7	12.0	-	11.0	47.7	-	-	-
5	42.3	25.8	21.8	-	10.1	-	-	-	-
6	1.8	0.5	1.2	-	-	96.5	-	-	-
7	41.7	21.4	21.2	-	-	15.8	-	-	-
8	3.5	1.5	3.4	-	11.1	80.5	-	-	-
9	36.4	21.7	20.3	-	-	17.1	4.5	-	-
10	4.1	1.8	2.2	-	11.6	80.3	-	-	-
11	47.0	20.9	23.8	-	1.3	-	-	7.0	-
12	9.7	6.7	7.7	-	9.3	65.8	-	-	-
13	46.6	21.4	27.4	-	-	-	-	-	4.6

Figure 3

Click here to access/download;Figure;Fig. 3.tif

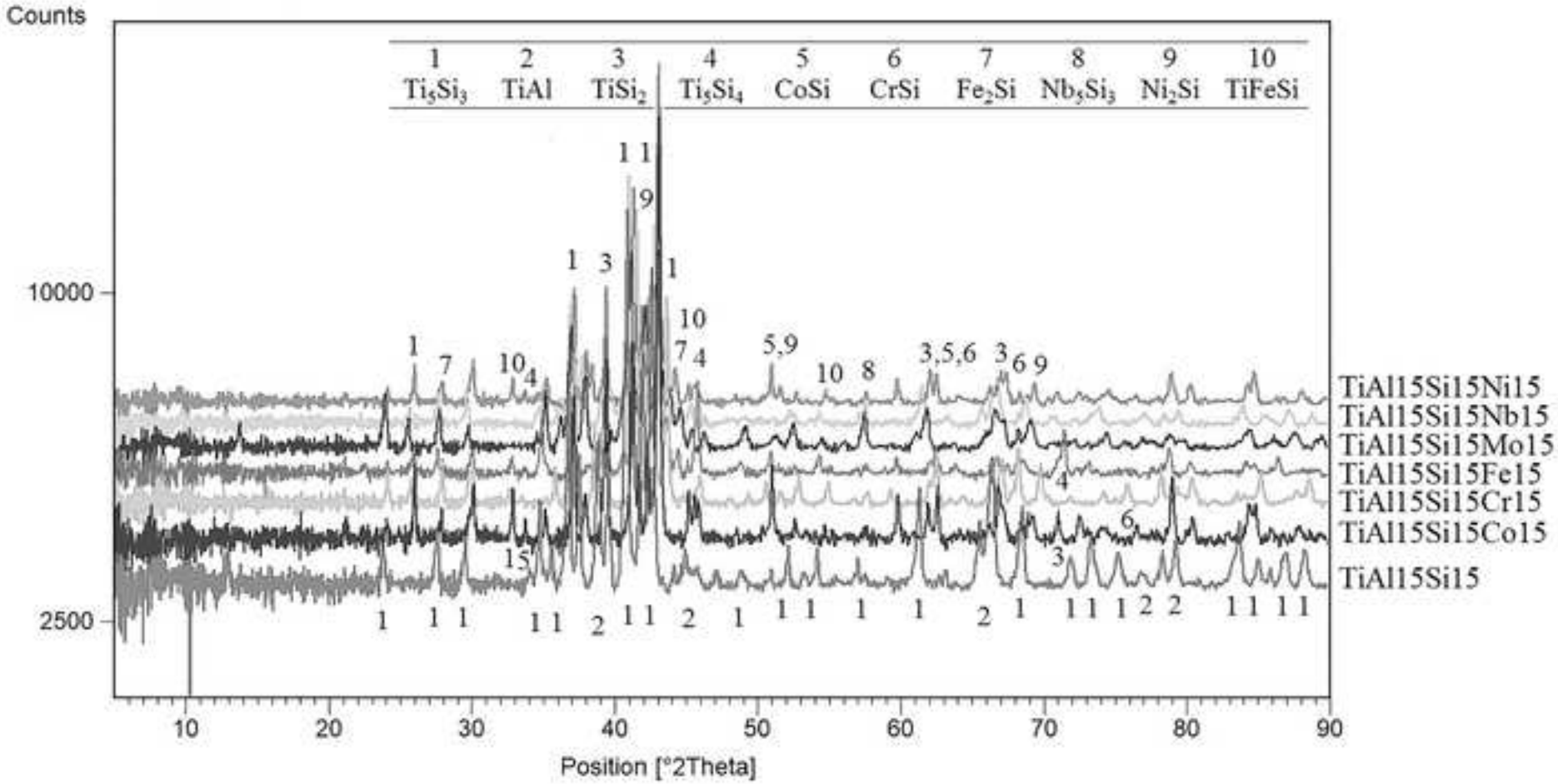

Alloy	Phases
TiAl15Si15Co15	Ti_5Si_3, $TiSi_2$, CoSi
TiAl15Si15Cr15	Ti_5Si_3, CrSi, TiAl
TiAl15Si15Fe15	Ti_5Si_3, Ti_5Si_4, TiAl
TiAl15Si15Mo15	Ti_5Si_3, Fe_2Si, TiAl
TiAl15Si15Nb15	Ti_5Si_3, $TiSi_2$, Nb_5Si_3, TiAl
TiAl15Si15Ni15	Ti_5Si_3, Ni_2Si, TiFeSi
TiAl15Si15	Ti_5Si_3, TiAl

Figure 4

Click here to access/download;Figure;Fig. 4.tif

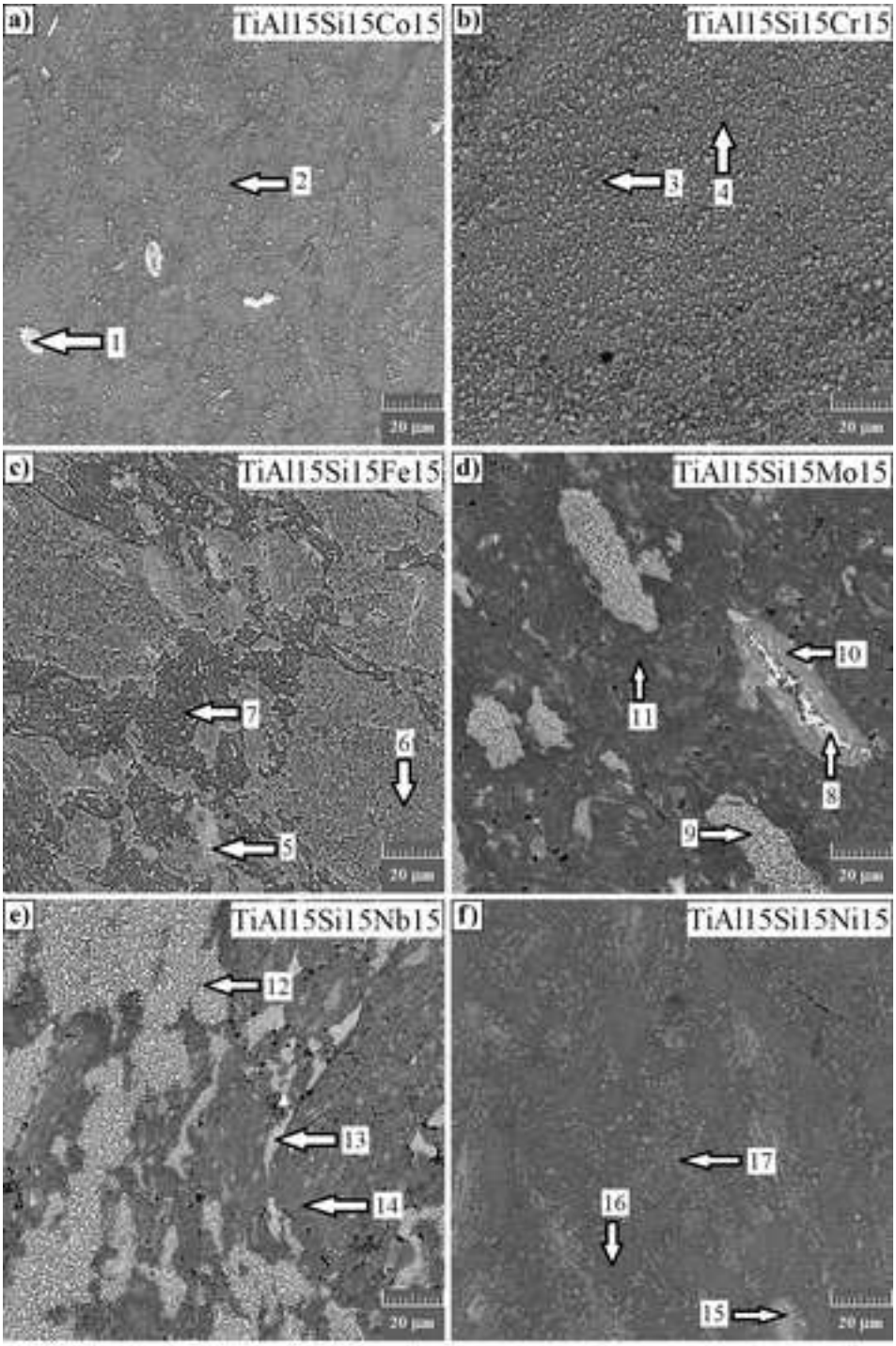

Spectrum	Ti	Al	Si	Co	Cr	Fe	Mo	Nb	Ni
1	35.0	14.8	17.1	8.3	3.5	21.3	-	-	-
2	48.1	20.2	24.4	7.4	-	-	-	-	-
3	52.2	13.9	22.7	-	11.2	-	-	-	-
4	42.1	28.0	19.4	-	10.5	-	-	-	-
5	38.0	16.5	19.9	-	-	25.7	-	-	-
6	44.8	15.2	24.2	-	-	15.8	-	-	-
7	39.1	24.7	20.8	-	-	15.4	-	-	-
8	16.4	12.9	10.9	-	-	58.4	1.5	-	-
9	49.7	12.2	25.8	-	-	6.3	6.0	-	-
10	27.7	5.9	17.9	-	-	45.2	3.2	-	-
11	51.3	23.5	22.3	-	-	-	2.9	-	-
12	47.2	14.9	20.6	-	-	11.4	-	5.8	-
13	39.5	11.7	17.7	-	-	25.6	-	5.6	-
14	40.2	23.7	17.8	-	-	10.1	-	8.1	-
15	37.0	14.1	19.0	-	-	22.8	-	-	7.2
16	47.2	21.6	25.1	-	-	-	-	-	6.1
17	40.2	15.7	27.1	-	-	12.3	-	-	4.7

Figure 5

Click here to access/download;Figure;Fig. 5.tif

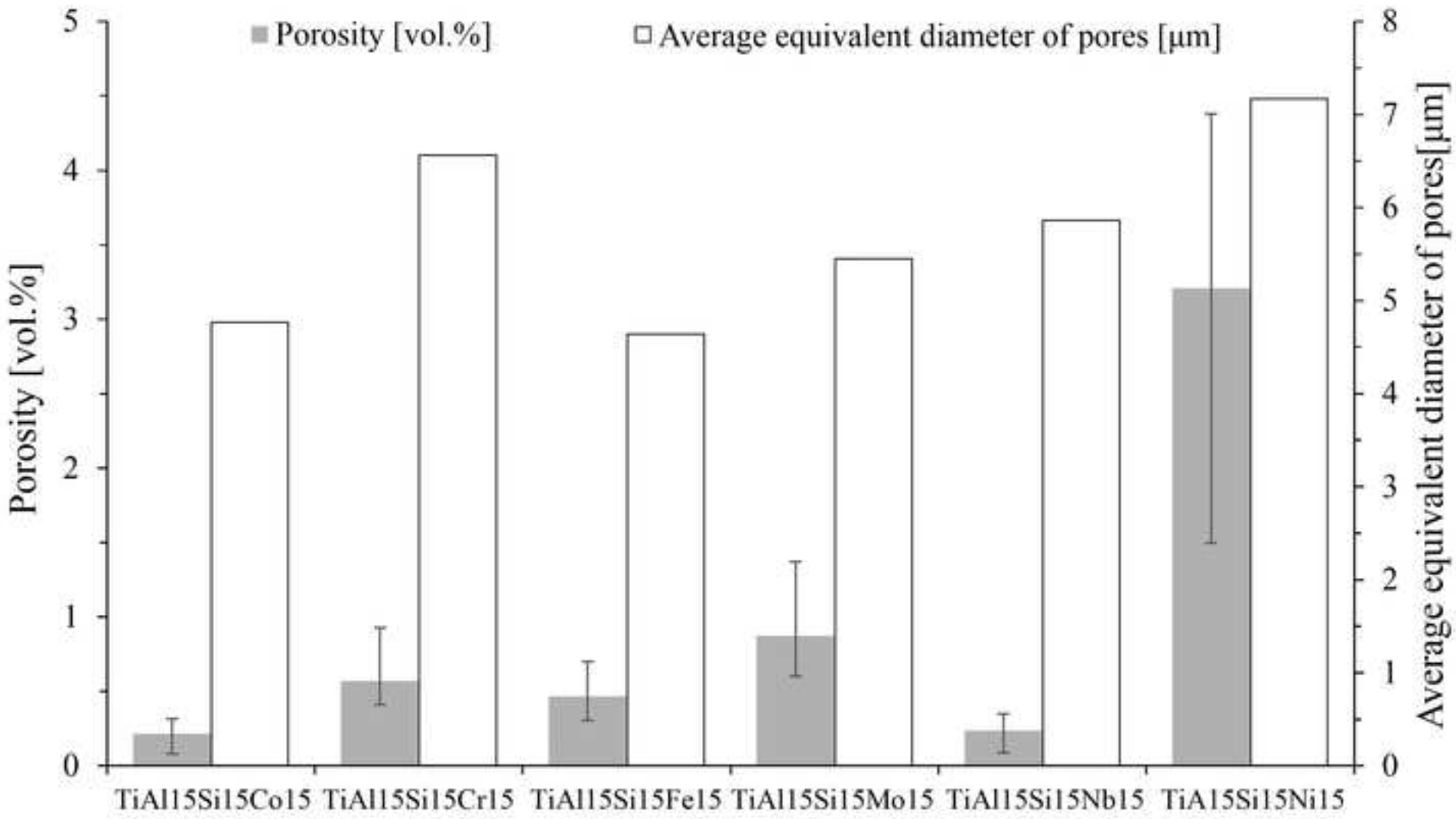

Figure 6

Click here to access/download;Figure;Fig. 6.tif

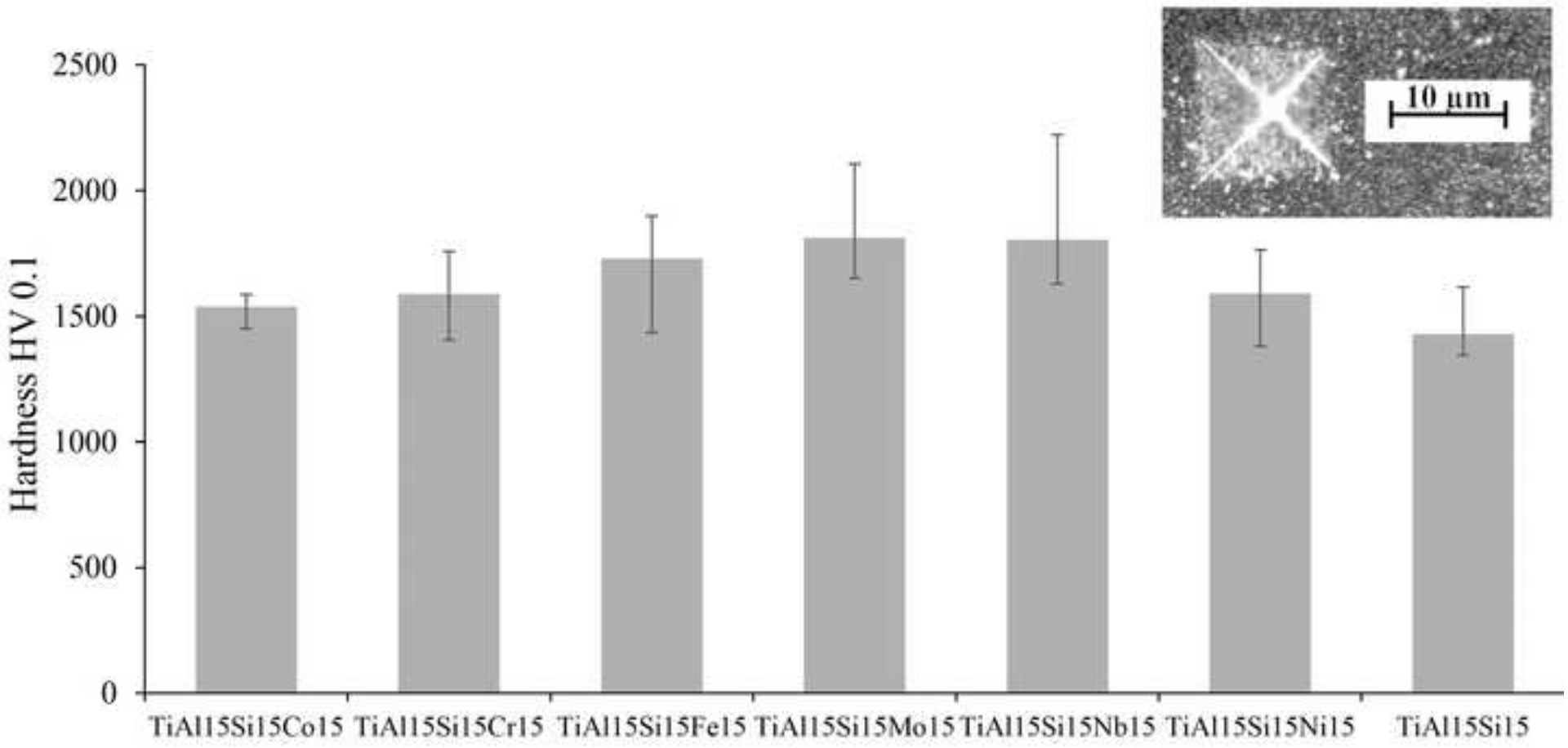

Figure 7

Click here to access/download;Figure;Fig. 7.tif

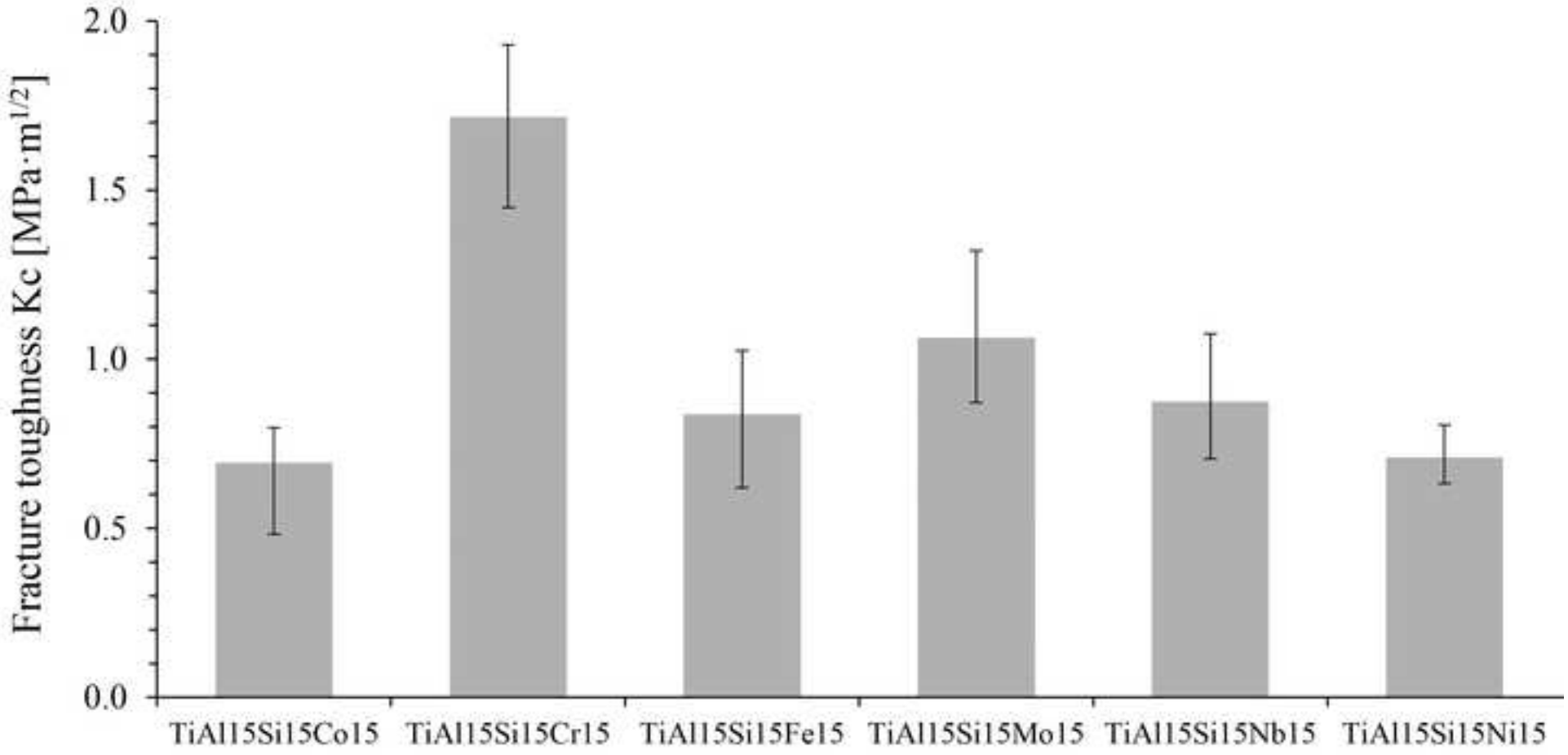

Figure 8

Click here to access/download;Figure;Fig. 8.tif

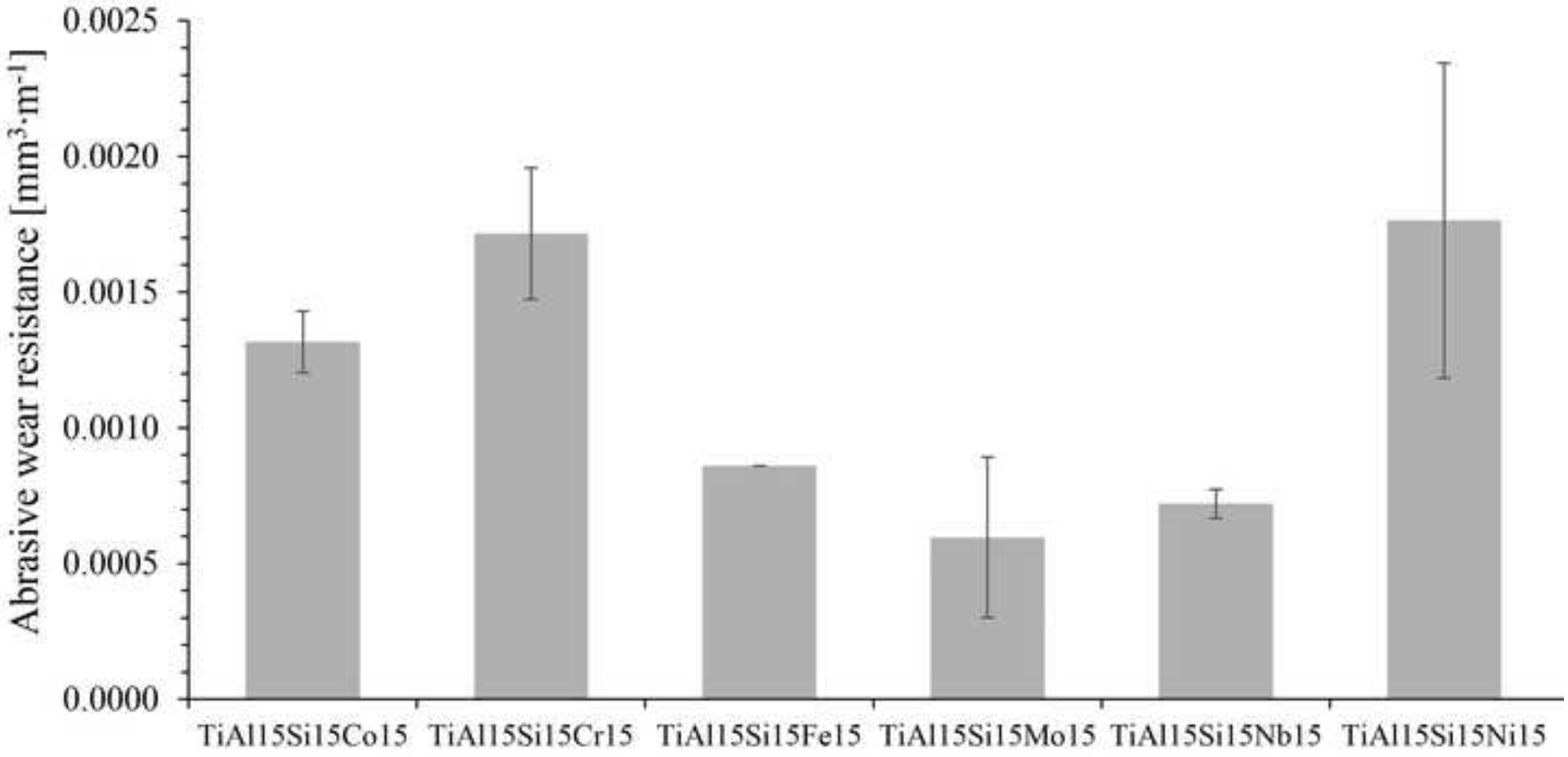

Figure 9

Click here to access/download;Figure;Fig. 9.tif

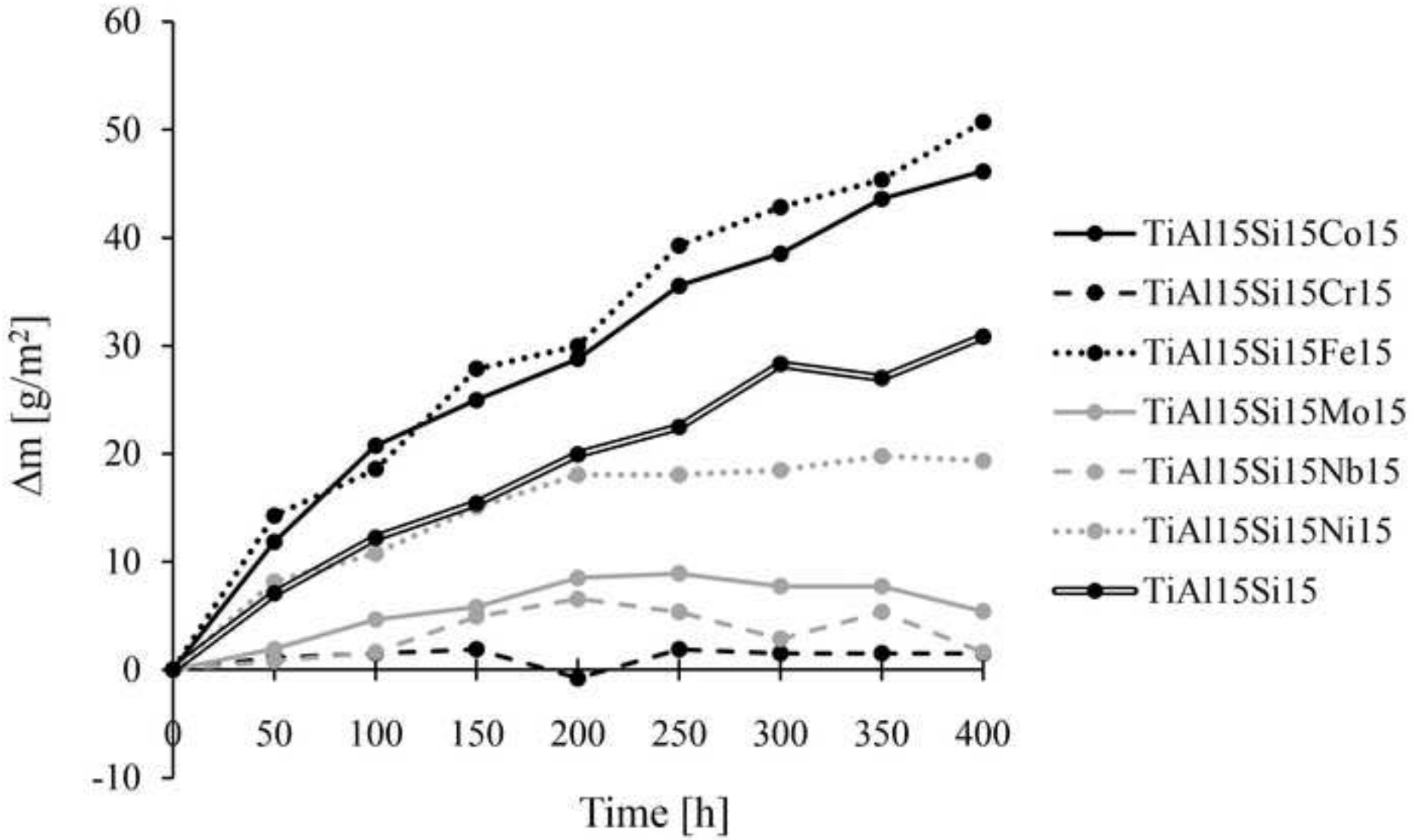

Figure 10

Click here to access/download;Figure;Fig. 10.tif

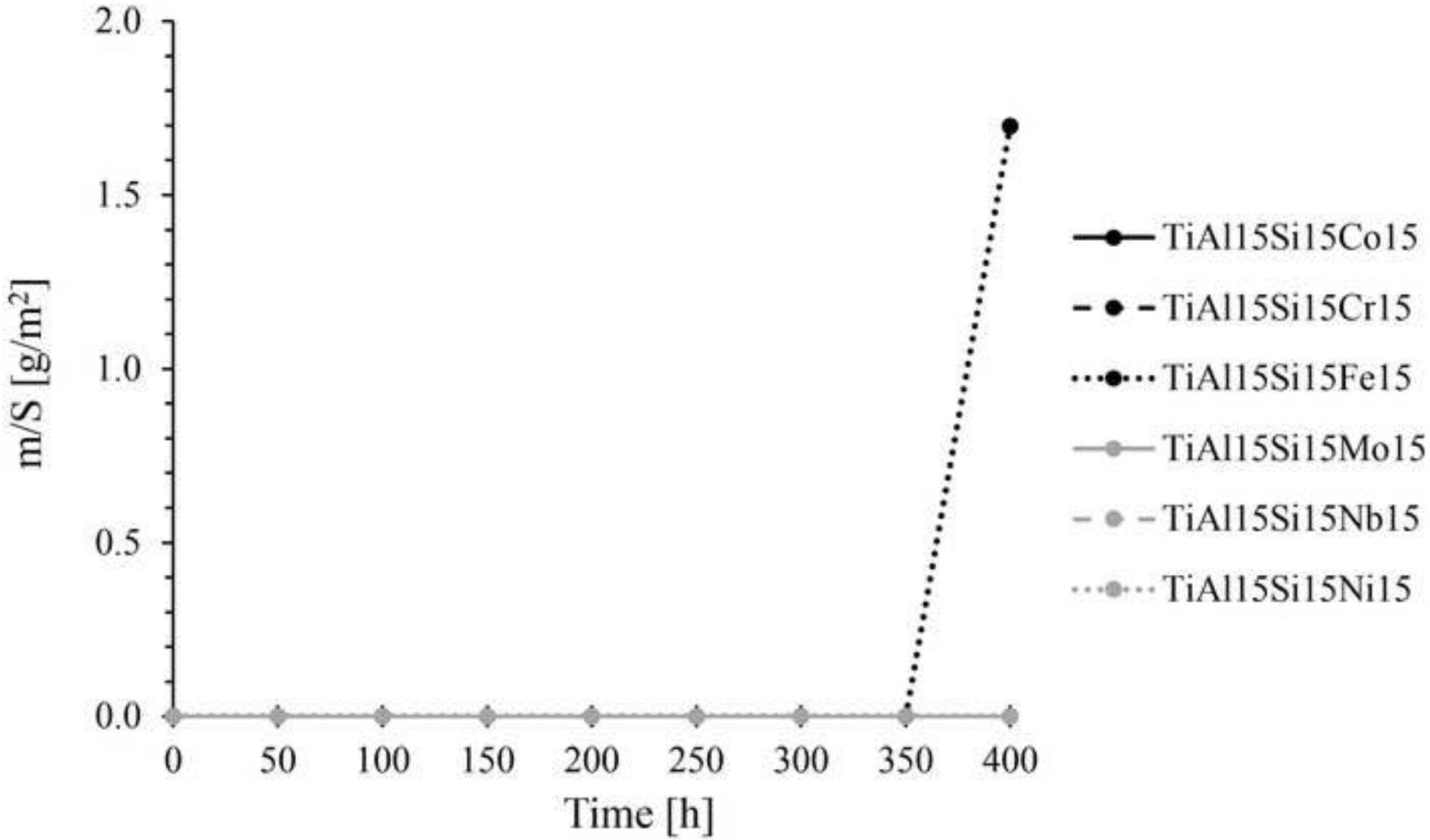

Figure 11

Click here to access/download;Figure;Fig. 11_.tif

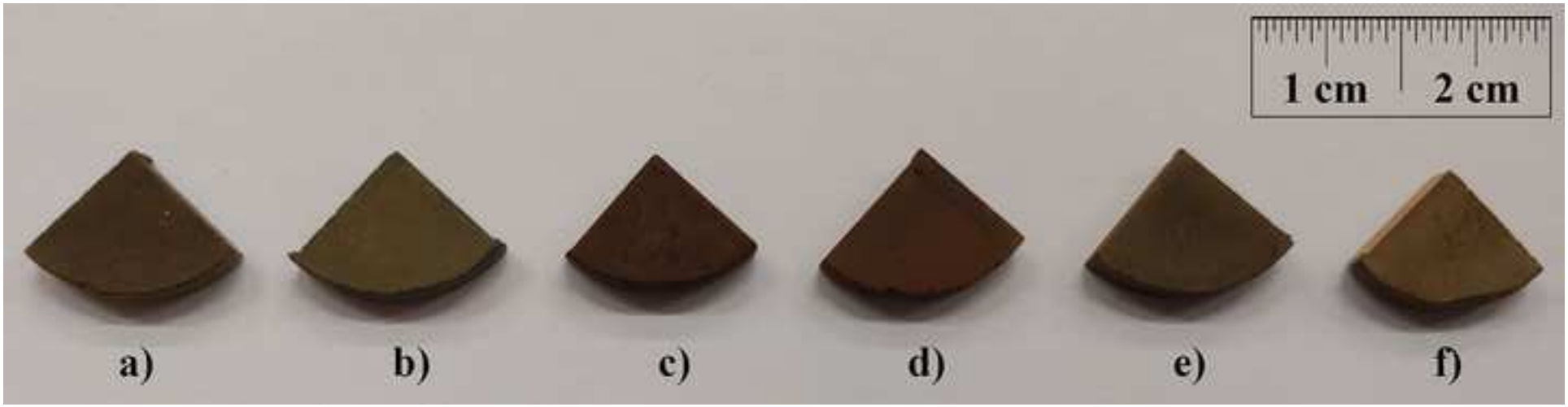

Figure 12

Click here to access/download;Figure;Fig. 12.tif

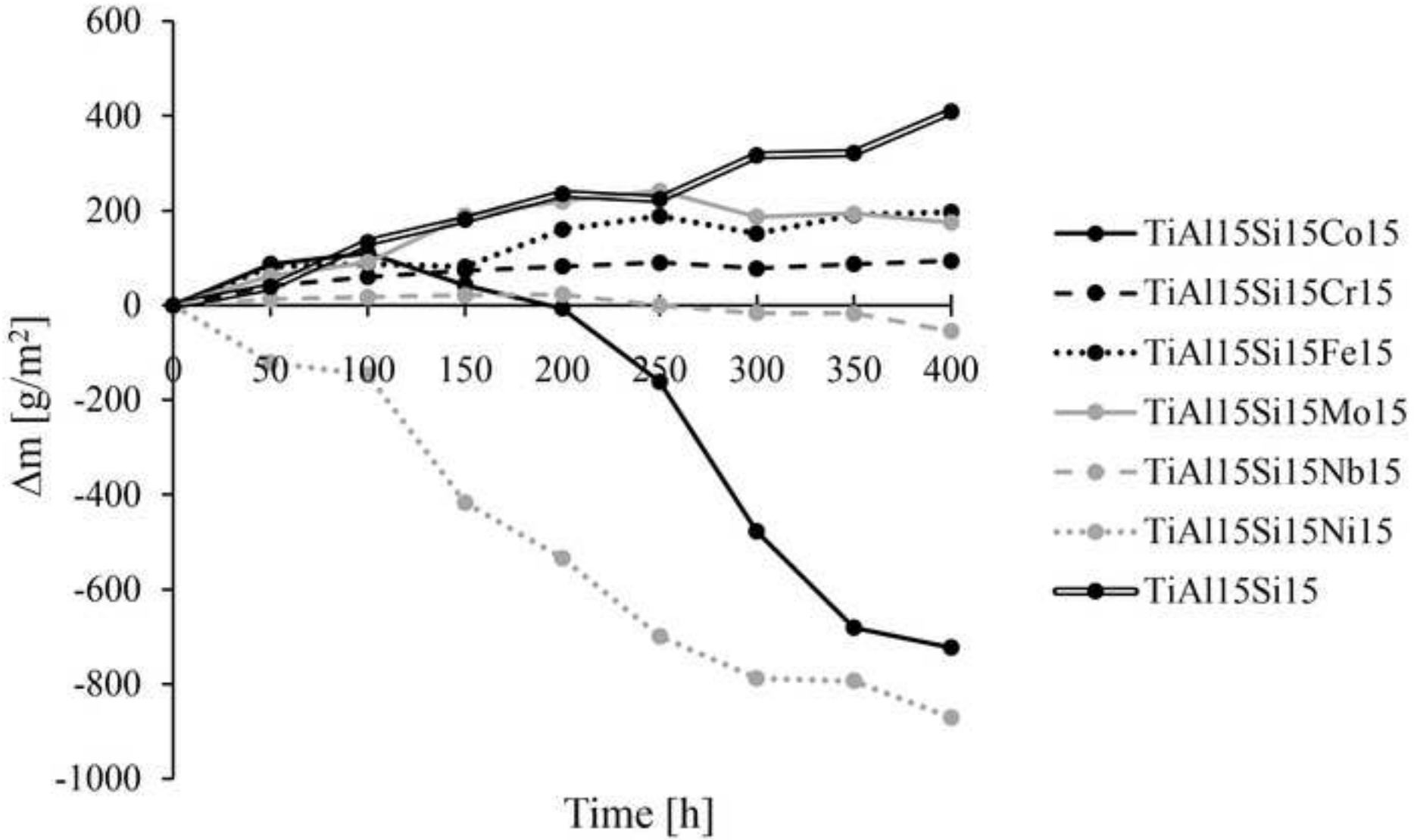

Figure 13

Click here to access/download;Figure;Fig. 13.tif

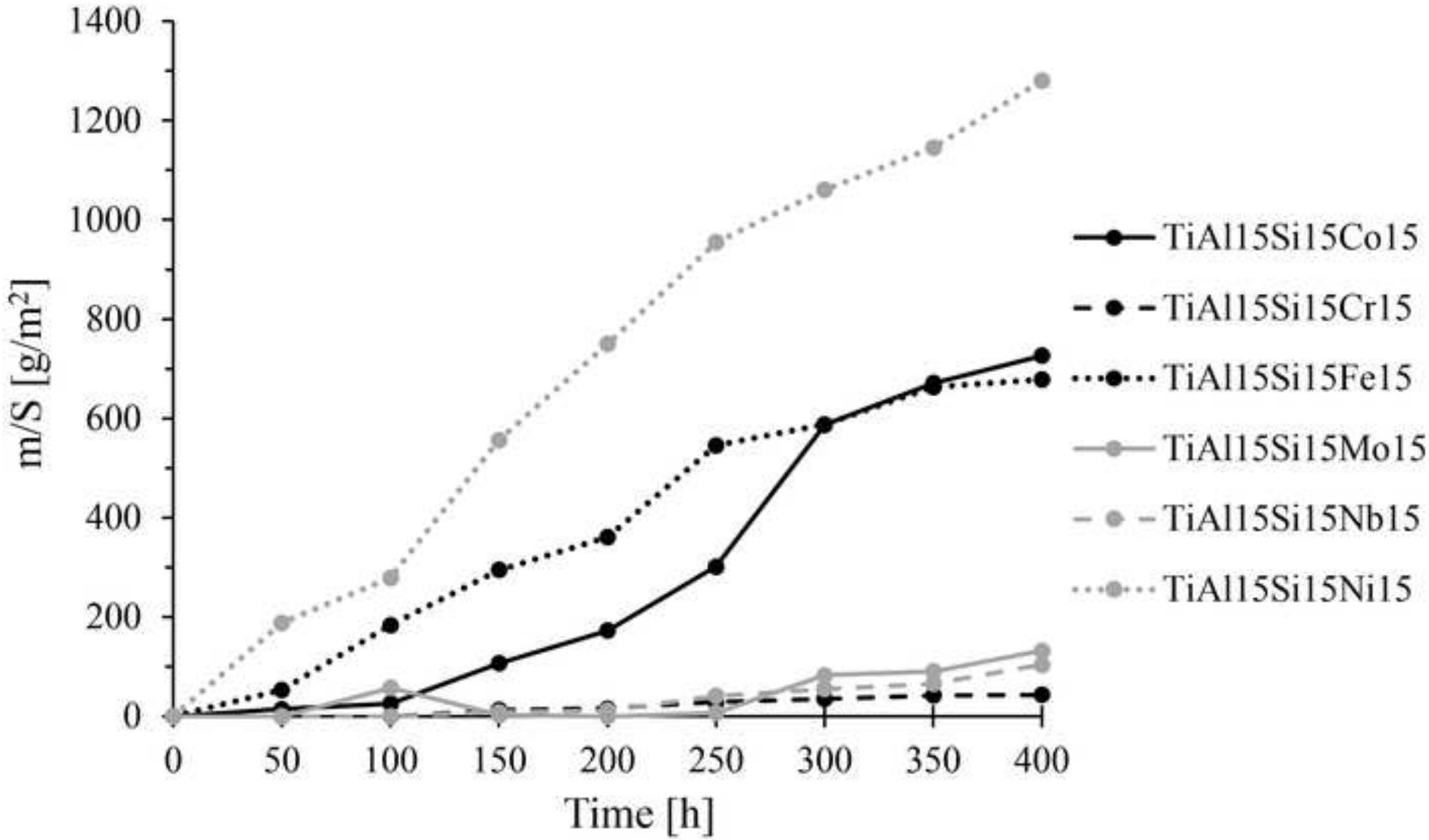

Figure 14

Click here to access/download;Figure;Fig. 14_.tif

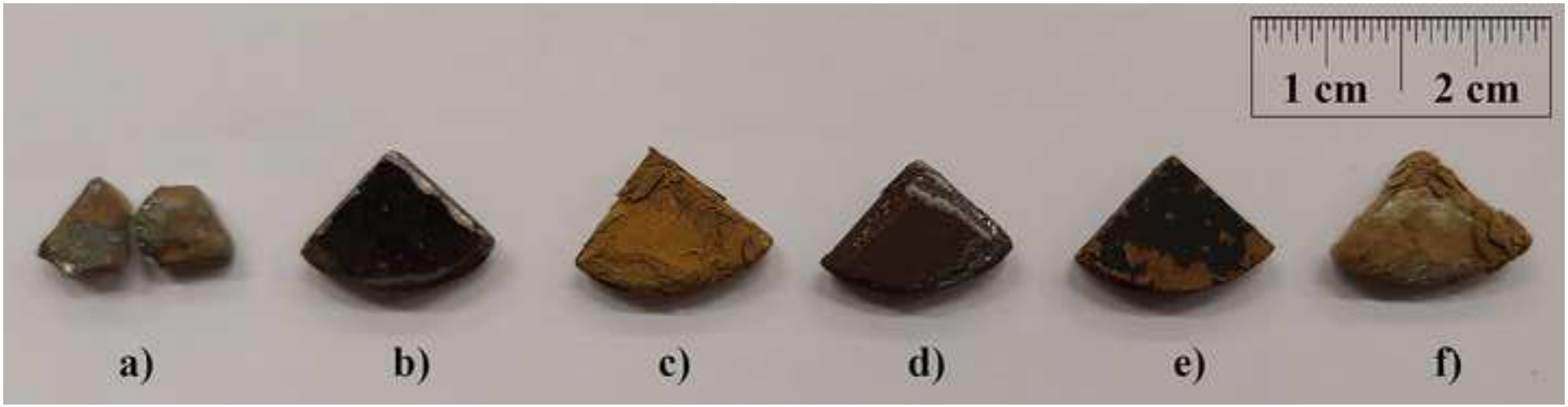

Figure 15

Click here to access/download;Figure;Fig. 15.tif

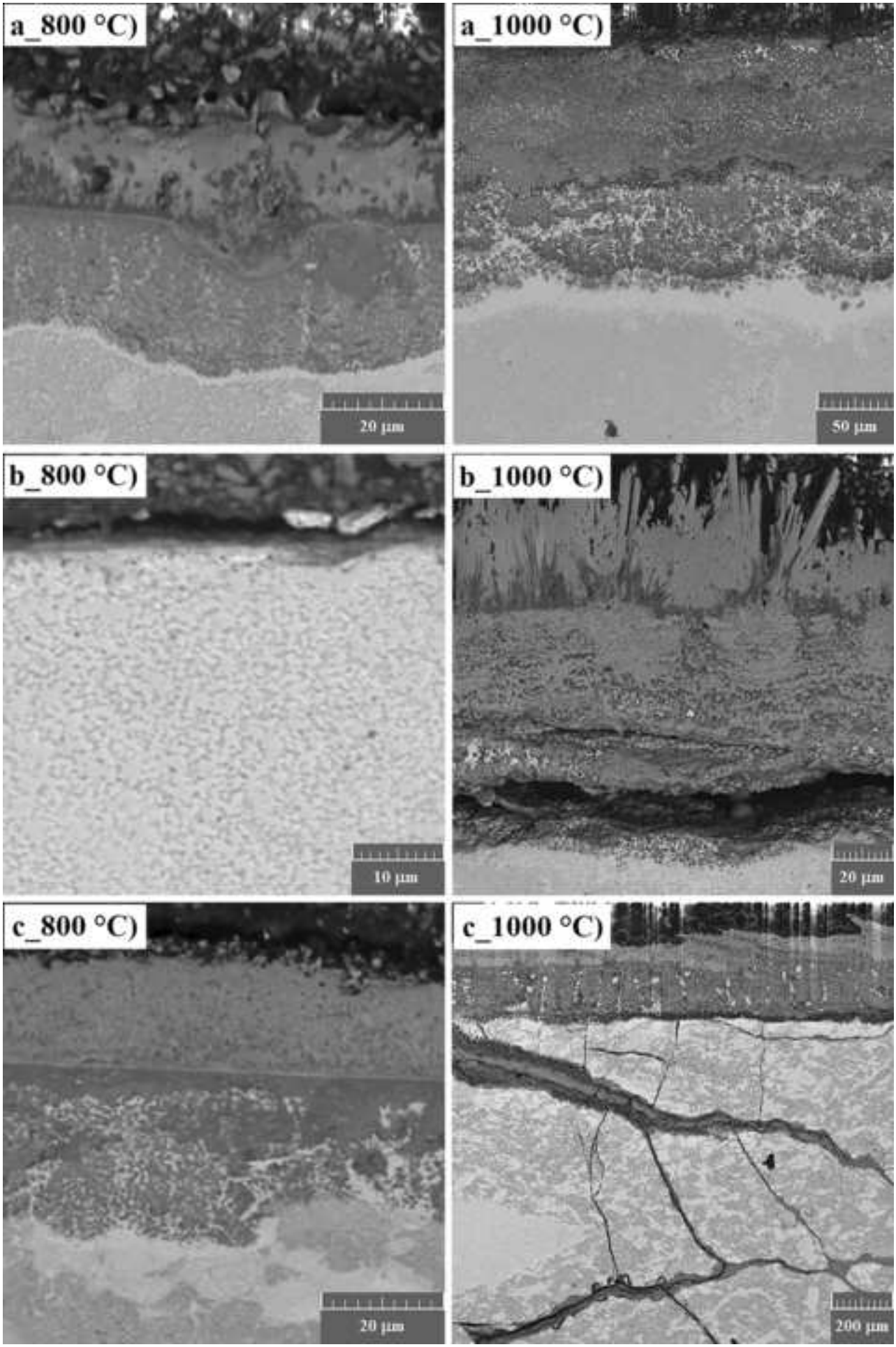

Figure 16

Click here to access/download;Figure;Fig. 16.tif

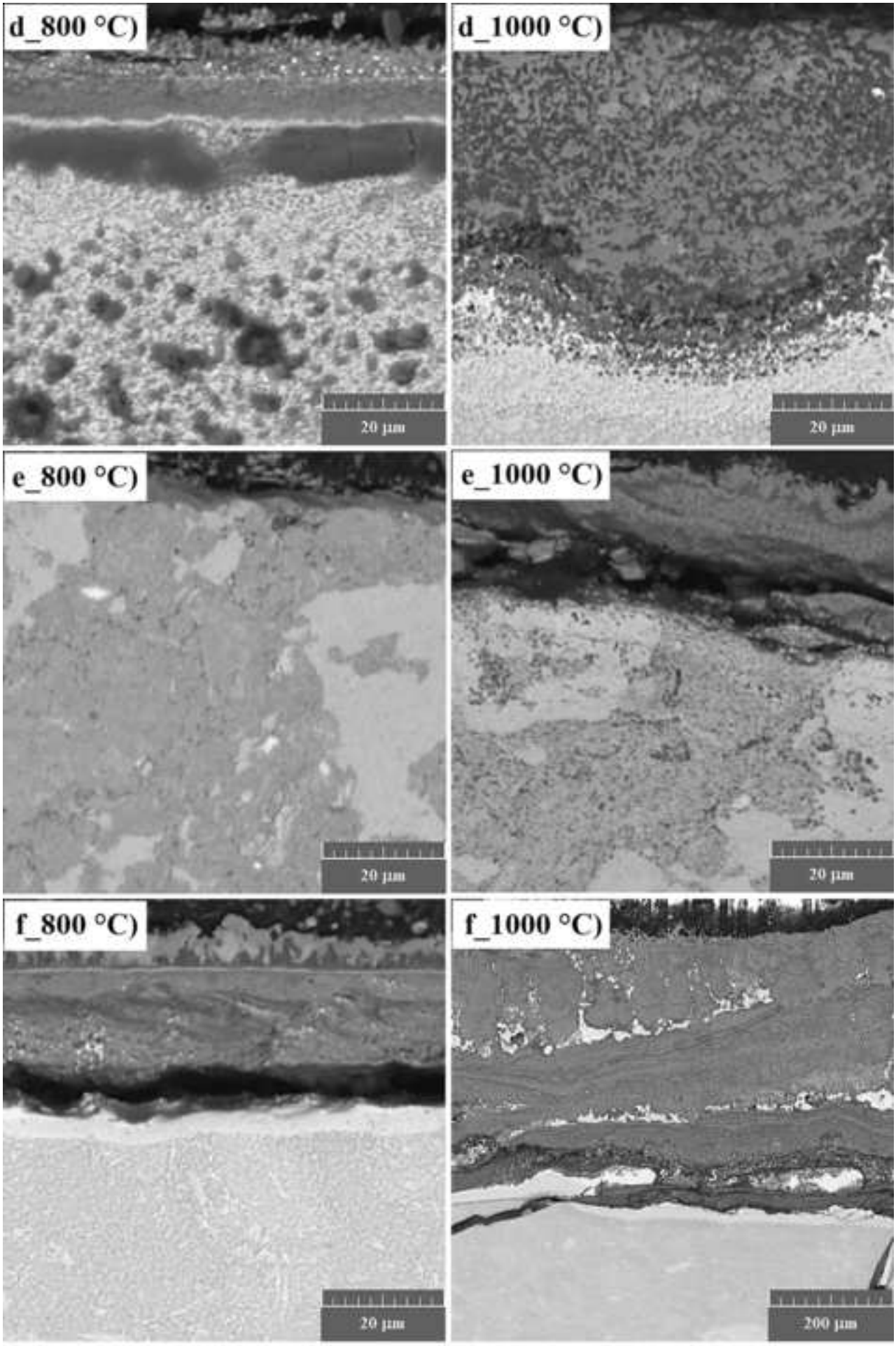

Figure 1

Click here to access/download;Figure;Fig. 1.tif

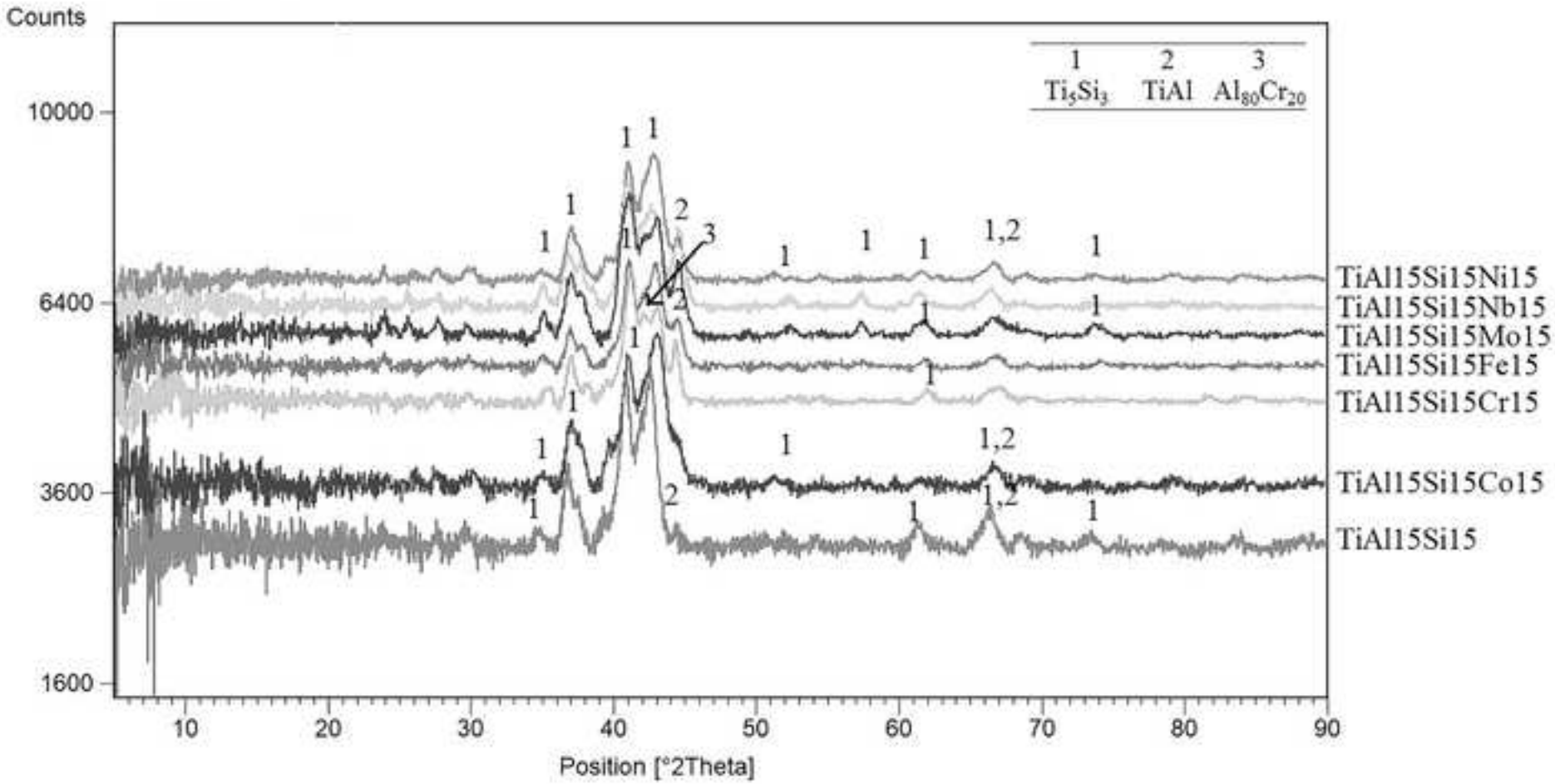

Credit Author Statement

Anna Knaislová: Methodology, Validation, Investigation, Data Curation, Writing - Original Draft

Vendula Šimůnková: Investigation, Data Curation

Pavel Novák: Conceptualization, Methodology, Validation, Data Curation, Writing - Review & Editing, Supervision

Filip Průša: Investigation

Marcello Cabibbo: Writing - Review & Editing

Lucyna Jaworska: Writing - Review & Editing

Dalibor Vojtěch: Resources, Supervision, Project administration, Funding acquisition

Declaration of interests

☒ The authors declare that they have no known competing financial interests or personal relationships that could have appeared to influence the work reported in this paper.

☐The authors declare the following financial interests/personal relationships which may be considered as potential competing interests:

Effect of alloying elements on the properties of Ti-Al-Si alloys prepared by powder metallurgy

Anna Knaislová[1*], Vendula Šimůnková[1], Pavel Novák[1], Filip Průša[1], Marcello Cabibbo[2], Lucyna Jaworska[3], Dalibor Vojtěch[1]

[1]Department of Metals and Corrosion Engineering, University of Chemistry and Technology, Prague. Technická 5, 166 28 Prague, Czech Republic.

[2]DIISM/Università Politecnica delle Marche, Via Brecce Bianche 12, 60131 Ancona, Italy.

[3]Department of Materials Science and Non-Ferrous Metals Engineering, AGH University of Science and Technology, al. Mickiewicza 30, 30-059 Krakow, Poland

*corresponding author, E-mail: knaisloa@vscht.cz

Abstract

Intermetallic alloys based on Ti-Al-Si system are significant for their excellent high-temperature properties, especially for resistance against oxidation and for achieving good mechanical properties at elevated temperatures. The main problem of these materials is high brittleness at room temperature. In the previous work, selected alloying elements were added into the Ti-Al-Si alloys prepared by reactive sintering, but the properties did not meet the requirements for subsequent use in the automotive or aerospace industry, since the materials had a very porous microstructure. Here, the addition of cobalt, chromium, iron, molybdenum, niobium and nickel into the TiAl15Si15 alloy prepared by mechanical alloying and Spark Plasma Sintering is tested and it is expected to improve the mechanical and high-temperature properties. In this paper, the Ti-Al-Si alloys have been assessed on basis of microstructure, phase composition, mechanical and tribological properties, such as hardness, fracture toughness and compressive strength. Cyclic oxidation tests were performed for 400 hours at the temperatures of 800 and 1000 °C. The cyclic oxidation tests simulate industrial processes, where the material is alternately exposed to elevated temperature and subsequent cooling (eg, engine components). From the viewpoint of most of the tested properties, alloying by niobium seems to be the most promising.

Keywords: intermetallics, mechanical alloying, sintering, microstructure, mechanical properties, oxidation

1. Introduction

Ti-Al-Si alloys consist of titanium aluminides and titanium silicides. Aluminide phases are tougher than silicide phases. On the other hand, silicides are very hard but brittle phases. Fracture toughness of TiAl phase at room temperature reaches from 11 to 18 MPa·m$^{1/2}$ and fracture toughness of Ti_5Si_3 reaches from 2 to 4 MPa·m$^{1/2}$ [1-8]. Ti-Al-Si alloys excel especially in low density, high-temperature oxidation and creep resistance [9-11]. The Ti_5Si_3 phase acts as a reinforcement for titanium aluminide matrix due to its strength, it is also very good chemically, and mechanically compatible with TiAl (they have similar thermal expansion coefficients) [12].

The previous studies have shown that aluminium and silicon in Ti-Al-Si alloys reduce the oxidation rate of titanium to approximately 850 °C. Resistance against high-temperature oxidation is caused by the formation of protective layers of TiO_2 (rutile), Al_2O_3 (corundum) and SiO_2 (silica). In particular, the addition of silicon has a significant reduction effect on the oxidation rate due to the slow rate of oxygen diffusion in the SiO_2 layer in comparison with the diffusion rate in rutile (TiO_2) [13, 14]. Silicon also supports the formation of TiN (titanium nitride) between the base material and the oxide layer, where it forms a separate layer or isolated particles reinforcing the base material. Silicon reduces the solubility and diffusion rate of nitrogen in the titanium, and thus the titanium nitride is not formed in the Ti-Al alloy [13, 15-17].

One of the main factors limiting the wider use of Ti-Al-Si alloys is their low fracture toughness at room temperatures due to the missing area of plastic deformation at the deformation curve [18]. The low fracture toughness is caused by the complex crystal structure of Ti_5Si_3 phase. Due to the low symmetry, the size of the Burgers vector is large in the Ti_5Si_3, raising the self energy of the dislocation. The low symmetry and highly covalent bonding, is responsible for a large Peierls stress, required for dislocation movement. As a result, even if dislocations are present inside the Ti_5Si_3 grains, they are hardly mobile. Another problem affecting the fracture toughness of Ti_5Si_3 is the coefficient of thermal expansion (CTE) anisotropy between the c and a axes, which generates thermal residual micro-stress inside the grains during cooling [8]. However, the plasticity of Ti-Al-Si alloys increases with the increasing temperature and can be improved by the addition of alloying elements. The upper limiting temperature of their use is set to 800 °C [19].

The addition of alloying elements (cobalt, chromium, iron, molybdenum, niobium and nickel) can improve strength, ductility and resistance to high-temperature oxidation of Ti-Al-Si alloys. There are few

comprehensive studies on the effect of alloying elements on this alloy system [10, 20, 21]. The addition of cobalt improves the high-temperature properties and hardness of these materials [22, 23], chromium improves ductility, strength and oxidation resistance and creep [24]. Iron atoms primarily substitute aluminium positions in TiAl, so they cause substitution strengthening [25]. Molybdenum and niobium increase high-temperature oxidation resistance and mechanical properties [22, 23, 26]. Niobium also improves the fracture toughness [23]. Niobium also increases the thermodynamic activity of aluminium compared to titanium and thus supports the formation of a stable Al_2O_3 layer. It also supports the formation of TiN layer at the interface between the oxide layer and the base material [27]. Nickel improves high-temperature properties [28].

The aim of this work is to describe the properties of TiAl15Si15X15 alloy (X = Co, Cr, Fe, Mo, Nb, Ni) prepared by mechanical alloying followed by Spark Plasma Sintering method. In this paper, microstructure, phase composition, selected mechanical and tribological properties and high-temperature oxidation behaviour are shown and the properties are compared with the ternary TiAl15Si15 alloy.

2. Material and methods

2.1. Preparation of intermediary phases by mechanical alloying and consolidation by Spark Plasma Sintering

Powders of intermetallic alloys TiAl15Si15X15 (wt. %), where X = Co, Cr, Fe, Mo, Nb, Ni, were prepared by powder metallurgy method using mechanical alloying. Pure powders were used as starting materials: titanium (purity 99.5 %, particle size < 50 μm), aluminium (purity 99.7 %, particle size < 50 μm), silicon (purity 99.5 %, particle size < 50 μm), cobalt (purity 99.8 %, particle size 2 μm), chromium (purity 99 %, particle size < 150 μm), iron (purity 99.9 %, particle size < 150 μm), molybdenum (purity 99 %, particle size < 150 μm), niobium (purity 99 %, particle size < 150 μm) and nickel (purity 99.99 %, particle size < 150 μm) powder. The prepared powder mixtures weighing 5 grams were placed in a milling vessel and mechanically alloyed in a planetary ball mill Retsch PM 100. Metal powders were ground with 10 milling balls (ball to powder ratio of approximately 60:1). The milling vessel made of 1.4034 stainless steel was filled by an inert gas (argon) to prevent the oxidation of powders. The parameters of mechanical alloying were chosen based on our previous research [12], the powders were milled 4 hours with 400 rpm and after 30 minutes the direction of rotation was changed.

Thus prepared powders were compacted by SPS (Spark Plasma Sintering). The sintering process was carried out at a temperature of 1100 °C for 15 minutes, a pressure of 80 MPa, in a continuous current flow mode and the resulting

tablets were cooled continuously with a rate of 50 °C/min. The resulting cylindrical sample had a height of 5 mm and a diameter of 20 mm.

2.2. Phase composition and microstructure of TiAl15Si15X15 alloys

The phase composition of milled powders, as well as compacted alloys, was examined by X-ray diffraction analysis by the means of a diffractometer PANalytical XPert Pro, diffraction patterns were evaluated in PANalytical HighScore plus program using the PDF2 database. The metallographic samples were prepared using grinding papers P80 to P4000, the ground samples were then polished with a polishing suspension Eposil F (a mixture of silica nanoparticles with hydrogen peroxide). The samples were etched by modified Kroll´s reagent (10 ml HF, 5 ml HNO_3 and 85 ml H_2O). The microstructure was observed using an optical light microscope Olympus PME3 with Carl Zeiss AxioCam ICc3 digital camera and AxioVision program. The detailed microstructure and the composition of individual phases of the samples was investigated by scanning electron microscope TESCAN VEGA 3 LMU equipped with energy dispersive analyser (SEM-EDS). The porosity and pore size were determined by microstructure images of non-etched compact alloys and evaluated by program Lucia 4.8.

2.3. Mechanical tests of TiAl15Si15X15 alloys

Mechanical properties were tested on the compacted alloys. Compressive strength tests were performed on a LabTest testing machine 5.250SP1-VM. The test specimens had the shape of a cube with an edge length of 3 mm. A minimum of 3 samples were tested for each alloy. Initial strain rate applied for compression testing was 2 mm·min^{-1}. Hardness and microhardness were measured using Vickers hardness with a load of 1 kg (HV 1) and 0.1 kg (HV 0.1) on the Future-Tech FM-700 machine. Fracture toughness was evaluated based on the crack size on the image analysis and determined by calculation according to Palmqvist equation (1):

$$K_c = 0.016 \cdot \left(\frac{E}{HV}\right)^{\frac{1}{2}} \cdot \left(\frac{F}{c^{\frac{3}{2}}}\right) \quad (1)$$

where Kc is the fracture toughness (MPa·m$^{1/2}$), E is the modulus of elasticity (GPa), HV is the Vickers hardness (HV 1, GPa), F is the load (N) and c is a half of crack length (mm). Abrasive wear resistance was carried out by a modified pin-on-disc method on a disc tribometer. Each tested sample passed approximately 2.5 km distance in 15 minutes on P1200 grinding paper with 5.8 N normal force. The position of the sample on the grinding paper was automatically changed continuously in order to keep the grinding ability of the paper for longer time. The resulting wear rate was calculated based on equation (2):

$$w = \frac{\Delta m}{\rho \cdot l} \quad (2)$$

where w is the wear rate ($cm^3 \cdot m^{-1}$), Δm is the mass loss (g), l denotes the path length on grinding paper (m) ρ is a density of sample ($g \cdot cm^{-3}$). The density was measured by the Archimedes method.

2.4. High-temperature oxidation tests of TiAl15Si15X15 alloys

Cyclic oxidation tests are intended to help simulate industrial processes where the material is exposed to elevated temperatures and subsequent cooling. The temperature of 800 °C was chosen according to the temperature of the applicability of Ti-Al alloys. The temperature of 1000 °C was chosen for the examination of the possibility of increasing the thermal stability by the addition of silicon. The alloy samples were annealed for 400 hours. The samples are removed from the furnace after 50-hours intervals, air-cooled, weighed and then returned to the furnace to the given temperature. The internal stress occurs between the base metal and its oxide layer as the consequence of cyclically repeated annealing. The sample and the sample with scaled-off oxides were weighed after every 50 hours. The oxide layer was observed using an optical and scanning electron microscope. The thickness of the oxide layer was measured by image analysis using ImageJ program. The values of parabolic constants were calculated according to equation (3):

$$K_p = \frac{\left(\frac{\Delta m}{A}\right)^2}{t} \quad (3)$$

where K_p ($g^2 \cdot m^4 \cdot h^{-1}$), Δm (g), A ($m^2$) and t (h) are the parabolic constant, the weight gain, the sample area and the duration of cyclic oxidation, respectively.

3. Results

3.1. Phase composition and microstructure of TiAl15Si15X15 powders

The optimal duration of mechanical alloying (MA) of TiAl15Si15X15 (X = Co, Cr, Fe, Mo, Nb, Ni) powders was chosen on the basis of the previous research [12]. After 4 hours of MA, all pure element powders have reacted and formed intermetallic phases. The phase composition of the mechanically alloyed powders is described by X-ray diffraction patterns in Figure 1. All alloys are formed by Ti_5Si_3 and TiAl stable phases. A metastable phase $Al_{80}Cr_{20}$ [29, 30] in TiAl15Si15Cr15 alloy is also formed. Furthermore, it can be assumed that all phases are substituted by other elements, as shown by the shift of the diffraction lines in the XRD pattern. With the mentioned exception of chromium, the alloying elements do not form separate phases but dissolve in titanium silicide or titanium aluminide.

The microstructure of TiAl15Si15X15 powders prepared by MA is shown in Fig. 2. Micrographs show that the powder particles have a homogeneous structure. Regions of different compositions are not visible, except for areas with higher amount of iron. All mechanically alloyed powders were contaminated by iron from the material of the milling vessel and balls - light areas in the figures. The particle size of alloy powder after MA varies in the order of tens of micrometres. Titanium with silicon form Ti_5Si_3 titanium silicide, titanium with aluminium form TiAl titanium aluminide. Because the phases are very fine and probably arose almost simultaneously during milling, silicon and aluminium in titanium silicide and aluminide are partially substituted by aluminium and silicon, respectively (see Spectrum in Fig. 2). Numerous cracks in the microstructure suggest the formation of brittle intermetallic phases.

3.2. Phase composition and microstructure of TiAl15Si15X15 compact alloys

Figure 3 shows the phase composition of TiAl15Si15X15 alloys prepared by mechanical alloying (MA) and Spark Plasma Sintering (SPS) using X-ray diffraction. All alloys are formed by Ti_5Si_3 titanium silicide, which is preferably formed because silicon has a high affinity to titanium. Silicides of alloying elements (cobalt, chromium, iron, niobium and nickel) are also present in the structure. The silicides are generally very hard and brittle phases. Titanium aluminides TiAl are also present in the alloy structure and they are tougher than silicides. Aluminides of other alloying elements were not identified as separate phases, although these elements (Co, Fe, Nb, Ni) form stable aluminides. It can be assumed that phases of unbalanced composition (i.e mixed aluminides and silicides), which are supersaturated over the equilibrium composition, are present in the structure of Ti-Al-Si-X alloys prepared by MA and SPS.

Figure 4 shows the microstructure of TiAl15Si15X15 (X = Co, Cr, Fe, Mo, Nb, Ni) alloys prepared by mechanical alloying followed by Spark Plasma Sintering. The microstructure is very fine-grained, well sintered and without the presence of unreacted basic elements. The structure of alloys consists of titanium silicides, selected silicides of alloying elements and titanium aluminide TiAl. Using the EDS point analysis elemental composition of various regions of microstructure was found. It cannot completely distinguish areas rich in individual phases. Because the phases are very fine, titanium silicide and aluminide are often substituted by aluminium and silicon, respectively (see Spectrum in Fig. 4). Individual areas of silicides of alloying elements (cobalt, chromium, niobium, nickel and iron) cannot be distinguished even by EDS analysis. Lighter areas indicate the presence of heavier elements such as iron or silicon. Darker areas appear

to be richer in aluminium. Numerous cracks were also detected in the microstructure of alloys, which are likely to arise due to anisotropy of the thermal expansion coefficient of Ti_5Si_3 phase in different crystal directions [9]. Iron contamination from the milling vessel and balls was found in all alloys.

The porosity of TiAl15Si15X15 alloys does not exceed 3 vol. % (Fig. 5). Alloy with nickel reaches the highest porosity. The remaining alloys reach the porosity under 1 vol. %. Average equivalent diameter of pores is from 4.5 to 7 µm (Fig. 5).

3.3. Mechanical and tribological tests of TiAl15Si15X15 compact alloys

The values of microhardness (HV 0.1) exceed 1500 HV 0.1 and range from 1527 HV 0.1 in the case of TiAl15Si15Co15 alloy up to 1813 HV 0.1 for TiAl15Si15Mo15 alloy (Fig. 6). Because the microstructure of the alloys is very fine-grained (see Fig. 6 top right, there is an indentation to TiAl15Si15Co15 alloy), it is possible to use a very small load to examine the hardness. The high values of microhardness of all alloys indicate significant reinforcement by alloying elements, in comparison TiAl15Si15 alloy described in our previous article [12] reached 1426 ± 136 HV 0.1. The hardness of Ti_5Si_3 titanium silicide and TiAl titanium aluminide were tested in our previous article [31]. Titanium silicide Ti_5Si_3 hardness varies between 1070 and 1175 HV 0.05, the hardness of the titanium aluminide varies between 200 and 530 HV 0.05. The big variations in the hardness of the aluminide phase are given by the substitution of silicon in titanium aluminide and the formation of small particles of titanium silicides in Ti-Al matrix. Titanium silicide Ti_5Si_4 has the same hardness as titanium silicide Ti_5Si_3 [31]. The values of microhardness correspond to phase composition described in Fig. 4. The highest values of microhardness were achieved by alloy with molybdenum and niobium. These elements are able to substitute titanium position in titanium aluminide (TiAl) and thus strengthen it significantly. And also the hardness of the niobium silicide Nb_5Si_3 is higher than the hardness of titanium silicide Ti_5Si_3 [32]. On the other hand, the microhardness value HV 0.1 of the TiAl15Si15Co15 alloy is the lowest of all alloys, because hardness of cobalt silicide CoSi is significantly lower than the hardness of titanium silicide Ti_5Si_3 [33].

Fracture toughness of all alloys is low, i.e. all alloys tend to brittle fracture (Fig. 7). The highest value of fracture toughness was reached by alloy with chromium (1.7 $MPa \cdot m^{1/2}$), the addition of chromium has a significant effect on the increase of toughness of titanium aluminides [22]. On the other hand, alloy with cobalt achieved the lowest value (0.69 $MPa \cdot m^{1/2}$) due to a higher portion of silicides, cracks and especially

pores in the microstructure, which behave as material imperfections. A stress concentration occurs at the edges of the microcrack. Then a certain stress value is reached, which leads to disruption of the bonds between atoms to form new surfaces [34].

The compression tests of Ti-Al-Si-X alloys were carried out at room temperature and the tests ended by fracture of material. There was no plastic deformation observed during the test, since the mechanically alloyed Ti-Al-Si-X alloys are brittle. The values of ultimate compressive strength vary for each alloy, mainly because of the occurrence of cracks and pores in the microstructure of alloys. The highest ultimate compressive strength was reached by TiAl15Si15Mo15 alloy (2298 MPa). Alloys containing niobium and iron exceeded the limit of 2000 MPa in at least one of the performed tests. The lowest ultimate compressive strength was reached by TiAl15Si15Co15 alloy due to the large number of structural inhomogenities (tab. 1).

Table 1 Ultimate compressive strength values of Ti-Al-Si-X alloys

Alloy	**Ultimate compressive strength [MPa]**
TiAl15Si15Co15	521
TiAl15Si15Cr15	1826
TiAl15Si15Fe15	2101
TiAl15Si15Mo15	2298
TiAl15Si15Nb15	2271
TiAl15Si15Ni15	1416

Ti-Al-Si-X alloys achieve very good values of abrasive wear resistance (Fig. 8). The wear rate of all alloys is very low, the lowest values were achieved by alloy with molybdenum, niobium and iron. The high abrasive wear resistance corresponds to the high ultimate compressive strength and hardness of these alloys.

3.4. High-temperature oxidation tests of TiAl15Si15X15 compact alloys

Fig. 9 shows the time dependence of the weight gain of Ti-Al-Si-X alloys during cyclic oxidation at 800 °C. It can be shown from the graph that the highest weight gain was found for alloys with cobalt and iron, but the values are minimal and comparable with tests of Ti-Al-Si alloys without alloying elements also prepared by MA+SPS [10]. On the contrary, an almost negligible weight gain was found in alloys with chromium and niobium, which confirmed the very positive effect of these elements on high-temperature

properties. The oxidation kinetics is probably controlled by a chemical reaction (linear course of the curve) for alloys with cobalt and iron, for others, it is a diffusion control (parabolic dependence). Fig. 10 shows the number of scaled-off oxides formed during cyclic oxidation at 800 °C. It can be seen from the graph that the amount of delaminated oxides is almost negligible for all alloys (the change in weight is in thousands of grams), which means that all oxide layers are cohesive and there is no peeling of oxides (which can be confirmed in Fig. 11, where the compact surface of each alloy is visible).

Fig. 12 shows the time dependence of the weight gain of Ti-Al-Si-X alloys during cyclic oxidation at 1000 °C. In the figure, it is possible to see the parabolic growth of the oxide layer in the case of an alloy with molybdenum, chromium, iron and niobium. In the sample of alloys with nickel and cobalt, there was a weight loss of the sample, which indicates the formation of no-adherent oxide layer, which delaminated during the oxidation test, as confirmed by Figures 13 and 14. The cobalt-alloyed alloy broke after 400 hours of oxidation (Fig. 14).

The phase composition of the oxide layer of Ti-Al-Si-X alloys was determined by X-ray diffraction analysis and the results are shown in tab. 2. The oxide layer consists of titanium dioxide (rutile), alumina (corundum) and silica. The oxide layer is also formed by oxides of alloying elements (MoO_2, MoO_3, Fe_2O_3) and mixed oxides (Al_2TiO_5, $FeTiO_3$). In addition to oxygen, nitrogen also penetrates from the air into the alloy, forming nitrides found in the alloy with iron (Fe_3N) and niobium (AlN, Nb_2N). In the alloy with molybdenum, niobium and nickel, aluminide and titanium silicide, which belong to the base material, were also detected in the oxide layer. These phases were found by X-ray diffraction because the oxide layer after oxidation at 800 °C is very thin and also a crack could be found at the diffraction site.

Table 2 Phase composition of the surface oxide layer of Ti-Al-Si-X alloys after 400 hours of cyclic oxidation

Alloy	**Phase composition (cyclic oxidation, 800 °C)**	**Phase composition (cyclic oxidation, 1000 °C)**
TiAl15Si15Co15	TiO_2, Al_2O_3, SiO_2	TiO_2, Al_2O_3, SiO_2
TiAl15Si15Cr15	TiO_2, Al_2O_3, SiO_2, Al_2TiO_5	TiO_2, Al_2O_3, SiO_2
TiAl15Si15Fe15	TiO_2, Al_2O_3, SiO_2, Fe_2O_3	TiO_2, Al_2O_3, SiO_2, Fe_3N, $FeTiO_3$
TiAl15Si15Mo15	TiO_2, Al_2O_3, MoO_3, Ti_5Si_3	TiO_2, SiO_2, MoO_2

TiAl15Si15Nb15	TiO_2, Al_2O_3, SiO_2, AlN, Ti_5Si_3	TiO_2, Al_2O_3, SiO_2, AlN, Nb_2N
TiAl15Si15Ni15	TiO_2, Al_2O_3, SiO_2, $TiAl_3$	TiO_2, Al_2O_3, SiO_2

The following Fig. 15 and Fig. 16 show the microstructure of the oxide layers of TiAl15Si15X15 alloys, the figure on the left always shows the appearance of the layer after oxidation at 800 °C, on the right after oxidation at 1000 °C. It can be seen from the figures that after oxidation at 800 °C, the alloy with cobalt, iron and nickel formed the thickest oxide layer, which was approximately 40 μm in thickness, while the alloy with chromium or niobium formed almost no observable oxide layer on the surface. For oxidation at 1000 °C, the results were similar, the alloys with cobalt, iron and nickel were the least resistant was again, while the alloys with chromium and niobium were the most resistant ones. The images show that some oxide layers are cracked. Cracks most often appear at the base material-oxide layer interface.

The elemental composition of individual parts of the oxide layer was determined by EDS analysis. The silicon and aluminium in Ti-Al-Si have a significant influence in improving the oxidation resistance of these alloys, which can reduce the activity of titanium atoms and suppress the formation of TiO_2. Silicon atoms also can react with titanium atoms to form stable titanium silicides [35].The outer part of the oxide layer is made of titanium dioxide, under which there are silica and alumina. The reasons for the formation of the silica and alumina mixed layer are (I) TiO_2 with faster growth rate restrained the formation of Al_2O_3, (II) the content of aluminium and silicon is limited, the content of aluminium for forming a protective scale is about 57–59 at. % [36] and the content of silicon for forming a protective scale must exceed 40 at.% [37-39]. In the inner part of the oxide layer, there is a higher proportion of alloying elements and we can also find selected oxides of iron or molybdenum. Using EDS analysis, no nitrogen-rich areas were found in any alloy.

4. Discussion

TiAl15Si15X15 alloys are all formed by the stable titanium silicide Ti_5Si_3 and silicides of the alloying elements (cobalt, chromium, iron, niobium and nickel). The aluminide matrix in all alloys is the TiAl phase, which is also found in the TiAl15Si15 alloy [12]. In articles [23, 40], TiAl15Si15X15 alloys were prepared by reactive sintering. The article described that some of the used alloying elements are mainly aluminide-forming (cobalt, copper and nickel), others silicide-forming (iron) and chromium with molybdenum form stable aluminides and silicides. SEM-EDS analysis showed that TiAl15Si15X15 alloys prepared by reactive

sintering do not form detectable amounts of silicides and aluminides of added alloying elements and only mixed silicides/aluminides are formed, where the alloying elements dissolve in titanium silicides and aluminides [10, 23]. TiAl15Si15X15 alloys in this work were prepared by mechanical alloying, where X-ray analysis of the powders did not show the formation of silicides or aluminides of the alloying elements after MA. After Spark Plasma Sintering, the formation of silicides of alloying elements (cobalt silicide CoSi, chromium silicide CrSi, iron silicide Fe_2Si, niobium silicide Nb_5Si_3 and nickel silicide Ni_2Si) was confirmed by X-ray diffraction. None of these silicides were found in samples prepared by reactive sintering. In the TiAl15Si15Fe15 alloy, a mixture of titanium aluminides TiAl and Ti_3Al was found after reactive sintering, while after MA+SPS only titanium aluminide TiAl was found. The results of the EDS analysis showed that the alloying elements do not form a detectable amount of their own phases during reactive sintering, they only dissolve in titanium silicides or aluminides. After SPS, the silicides of the alloying elements arose.

Mechanical alloying causes aluminium in titanium aluminides to be strongly substituted with silicon and vice versa in titanium silicides. The authors described that Ti(Al,Si) supersaturated solid solutions are formed after at least 10 to 20 hours of milling [41, 42], but as shown in this work, intermetallic phases are formed during a much shorter mechanical alloying duration (after 4 hours). Mechanical alloying in combination with Spark Plasma Sintering leads to a very fine microstructure of the investigated alloys. The authors described that mechanical alloying is a very efficient process for obtaining nanometer-sized grains [43, 44]. The refinement of Ti_5Si_3 crystallites is probably due to strong deformation and subsequent recrystallization. The distribution of titanium silicides is much more homogeneous because the brittle powder is crushed into very fine particles during the first step of the mechanical alloying. The elements in the obtained compounds are substituted for each other, which exceeds the limits of equilibrium solubility [45]. Fine-grained microstructure due to mechanical alloying and higher compaction pressure significantly reduced the porosity of alloys compared to alloys prepared by reactive sintering [23]. The porosity of the TiAl15Si15 alloy prepared by MA+SPS was 0.4 % by volume [12]. The addition of chromium and molybdenum slightly increased the porosity (to 0.7 % by volume and 0.8 % by volume, respectively), the addition of iron tripled the value (to 1.2 % by volume) and the addition of cobalt even increased fivefold (to 2 % by volume). The same effect of these alloying elements is also mentioned in articles [23, 40]. The article [23] further shows that the addition of nickel reduces the porosity, however, the opposite effect was found in

this work. The TiAl15Si15Ni15 alloy had the same high porosity value as the alloy with cobalt. Only niobium as an alloying element did not increase the porosity, the TiAl15Si15Nb15 alloy had the same porosity as the TiAl15Si15 alloy without alloying elements.

The values of microhardness correspond with the phase composition of alloys. The microhardness values of all TiAl15Si15X15 alloys are higher than the values for the TiAl15Si15 alloy prepared by MA+SPS [31] because the alloys were further strengthened by the addition of alloying elements. Also, the increase in hardness may be associated with the strengthening of hard particles of titanium silicides by alloying elements [23]. The values of microhardness correspond with phase composition described in Fig. 4. The highest values of microhardness were achieved by alloy with molybdenum and niobium. Molybdenum and niobium substitute the positions of titanium in titanium aluminide TiAl, thus significantly strengthening it, so the microhardness of these alloys was the highest of all tested. These elements are able to substitute titanium position in titanium aluminide (TiAl) and thus strengthen it significantly. And also the hardness of the niobium silicide Nb_5Si_3 is higher than the hardness of titanium silicide Ti_5Si_3 [32]. On the other hand, the microhardness value HV 0.1 of the TiAl15Si15Co15 alloy is the lowest of all alloys, because hardness of cobalt silicide CoSi is significantly lower than the hardness of titanium silicide Ti_5Si_3 [33]. Along with the hardness, the alloying elements also increased the ultimate compressive strength values, except for the alloy with cobalt or nickel, where there were numerous cracks in the microstructure. The article [40] shows that all alloying elements added to Ti-Al-Si alloys prepared by reactive sintering decrease mechanical properties, especially fracture toughness. In our case, however, the fracture toughness did not decrease, on the contrary, the fracture toughness reached higher values comparable to TiAl15Si15 alloy without alloying elements [31]. The TiAl15Si15Cr15 alloy prepared by ML + SPS reached the best values of fracture toughness of all tested alloys. However, the fracture toughness of all tested alloys is low, even lower than can be expected from the combination of reported values for titanium aluminide and silicide phase (see above). The reason is probably in the formation of high amount of defects during mechanical alloying, which results in massive deformation strengthening, but also a drop of the toughness. Hence, mechanical alloying cannot be recommended as the manufacturing method from the viewpoint of fracture toughness.

On the contrary to toughness, the wear resistance is one of the key strengths of the tested alloys. When we compare the achieved values, they are comparable with the plasma nitrided alloyed high-carbon tool steel,

which was recently tested under the same conditions [46]. The wear resistance was the best in the case of the iron-, molybdenum- and niobium-containing alloys, i.e. in the case of elements, which form and could enter the M_5Si_3 silicides. So the stabilization and possible strengthening of the silicide phase has the key effect on the wear resistance. Due to high wear resistance, the tested alloys can be considered as candidates for the protective coating used under the conditions of high abrasive wear.

The high-temperature oxidation can be controlled by diffusion or chemical reactions. If the growth of the oxide layer proceeds through a diffusion-controlled mechanism, the resulting growth of the oxide layer to the annealing time has a parabolic dependence. During the oxidation, the oxide layer grows to a certain limit, where the diffusion of oxygen into the material is limited. The layer on the material no longer grows, so it protects the material well. The linear dependence of the kinetic curve is associated with the formation of an oxide layer by chemical reaction-controlled process. This mechanism applies primarily when the material has a porous oxide layer or contains a significant amount of cracks, and so oxygen from the surrounding atmosphere can easily penetrate into the depth of the material. Likewise, this mechanism applies to the destroying of the oxide layer (pores, cracks). The formation of the oxide layer can be determined based on values of parabolic constant Kp. If the value of the parabolic constant does not change over time, it indicates the diffusion-controlled mechanism. The high-temperature behaviour of Ti-Al-Si alloys was detailed described in our previous articles [10, 19, 47, 48].

The authors described that the high-temperature behaviour of Ti-Al-Si alloys can be improved by the addition of other alloying elements. The addition of niobium was the most studied [49-54]. The combination of silicon and niobium resulted in much better oxidation resistance than with the addition of individual elements. Cobalt, chromium, copper, iron, molybdenum and nickel also increase the resistance to oxidation at 1000 °C [23]. In this article [23] the Ti-Al-Si-based alloy prepared by reactive sintering and containing 15 wt. % molybdenum had the best oxidation resistance, followed by an alloy with chromium. These two alloys also showed very good thermal stability [23, 40]. The positive influence of alloying elements for the oxidation resistance of Ti-Al-Si alloys was also confirmed in this work. All alloys had very good adhesion of the oxide layer, which was relatively thin, and the minimum scaled-off oxides occurred only at a temperature of 1000 °C. The most oxidation-resistant samples were alloyed with chromium and niobium, which confirms the positive effect of these elements on oxidation resistance.

5. Conclusions

Ti-Al-Si alloys prepared by mechanical alloying have a homogeneous and fine-grained microstructure with low porosity, which ensures high mechanical properties. Ti-Al-Si alloys are extremely resistant at temperatures up to 800 °C. The addition of alloying elements improved the properties of Ti-Al-Si alloys. Along with hardness, the alloying elements also increased the compressive strength values. The TiAl15Si15Cr15 alloy achieved the best values of fracture toughness of all tested alloys. However, the values of toughness are still too low. The best oxidation resistance was achieved by an alloy with niobium and chromium. The presented results indicate that the tested alloys could be applicable e.g. in the form of protective coatings, where the excellent high-temperature oxidation and wear resistance can be utilized.

Acknowledgement

This work was supported from the grant of Specific university research – grant No A1_FCHT_2020_003 and A2_FCHT_2020_046.

References

[1] A. Kakitsuji, J. Ramkumar, J. Kinose, H. Mabuchi, H. Tsuda, K. Morii, Synthesis of TiAl(Cr)/Ti2AlC Composites by Reactive Arc-Melting, Materials Transactions - MATER TRANS, 43 (2002) 2589-2592.

[2] K.S. Min, A.J. Ardell, S.J. Eck, F.C. Chen, A small-specimen investigation of the fracture toughness of Ti5Si3, Journal of Materials Science, 30 (1995) 5479-5483.

[3] K. Kasraee, M. Yousefpour, S.A. Tayebifard, Microstructure and mechanical properties of Ti5Si3 fabricated by spark plasma sintering, Journal of Alloys and Compounds, 779 (2019) 942-949.

[4] K. Kasraee, M. Yousefpour, S.A. Tayebifard, Mechanical properties and microstructure of Ti5Si3 based composites prepared by combination of MASHS and SPS in Ti-Si-Ni and Ti-Si-Ni-C systems, Materials Chemistry and Physics, 222 (2019) 286-293.

[5] D. Gu, W. Meiners, C. Li, Y. Shen, In situ synthesized TiC/Ti5Si3 nanocomposites by high-energy mechanical alloying: Microstructural development and its mechanism, Materials Science and Engineering: A, 527 (2010) 6340-6345.

[6] K. Kothari, R. Radhakrishnan, N.M. Wereley, T.S. Sudarshan, Microstructure and mechanical properties of consolidated gamma titanium aluminides, Powder Metallurgy, 50 (2007) 21-27.

[7] J. Ramkumar, A. Kakitsuji, S.K. Malhotra, R. Krishnamurthy, H. Mabuchi, H. Tsuda, T. Matsui, K. Morii, Mechanical and Erosion Behaviour of Ti47Al-3W/TI2ALC Composites by Reactive Arc-Melting, 12 (2003) 096369350301200402.

[8] R. Mitra, N. Eswara Prasad, Y.R. Mahajan, Mechanical behaviour of Ti5Si3 based alloys and composites, Transactions of the Indian Institute of Metals, 61 (2008) 427-433.

[9] N.S. Stoloff, V.K. Sikka, Physical metallurgy and processing of intermetallic compounds, Chapman & Hall, 1996.

[10] A. Knaislová, P. Novák, F. Průša, M. Cabibbo, L. Jaworska, D. Vojtěch, High-temperature oxidation of Ti–Al–Si alloys prepared by powder metallurgy, Journal of Alloys and Compounds, 810 (2019) 151895.

[11] A. Lasalmonie, Intermetallics: Why is it so difficult to introduce them in gas turbine engines?, Intermetallics, 14 (2006) 1123-1129.

[12] A. Knaislová, J. Linhart, P. Novák, F. Průša, J. Kopeček, F. Laufek, D. Vojtěch, Preparation of TiAl15Si15 intermetallic alloy by mechanical alloying and the spark plasma sintering method, Powder Metallurgy, 62 (2019) 56-60.

[13] P. Novák, Příprava, vlastnosti a použití intermetalických sloučenin, Chemické listy, 106 (2012) 884-889.

[14] N.S. Stoloff, C.T. Liu, S.C. Deevi, Emerging applications of intermetallics, Intermetallics, 8 (2000) 1313-1320.

[15] R. Nesper, Intermetallics. Von G. Sauthoff. VCH Verlagsgesellschaft, Weinheim, 1995. 165 S., geb. 128.00 DM. – ISBN 3-527-29320-5, Angewandte Chemie, 108 (1996) 726-727.

[16] D. Shi, B. Wen, R. Melnik, S. Yao, T. Li, First-principles studies of Al–Ni intermetallic compounds, Journal of Solid State Chemistry, 182 (2009) 2664-2669.

[17] C.L. Yeh, H.J. Wang, W.H. Chen, A comparative study on combustion synthesis of Ti–Si compounds, Journal of Alloys and Compounds, 450 (2008) 200-207.

[18] A. Knaislová, P. Novák, M. Cabibbo, F. Průša, C. Paoletti, L. Jaworska, D. Vojtěch, Combination of reaction synthesis and Spark Plasma Sintering in production of Ti-Al-Si alloys, Journal of Alloys and Compounds, 752 (2018) 317-326.

[19] A. Knaislová, V. Šimůnková, P. Novák, F. Průša, High-temperature behaviour of Ti-Al-Si alloys prepared by Spark Plasma Sintering, Manufacturing Technology, 17 (2017) 733-738.

[20] P. Novák, F. Průša, J. Šerák, D. Vojtěch, A. Michalcová, Oxidation resistance and thermal stability of Ti-Al-Si alloys produced by reactive sintering, Metal, (2009).

[21] X. Lu, X.B. He, B. Zhang, X.H. Qu, L. Zhang, Z.X. Guo, J.J. Tian, High-temperature oxidation behavior of TiAl-based alloys fabricated by spark plasma sintering, Journal of Alloys and Compounds, 478 (2009) 220-225.

[22] G. Sauthoff, Intermetallics, VCH, Weinheim, New York, Basel, Cambridge, Tokyo, 1995.

[23] P. Novák, J. Kříž, F. Průša, J. Kubásek, I. Marek, A. Michalcová, M. Voděrová, D. Vojtěch, Structure and properties of Ti–Al–Si-X alloys produced by SHS method, Intermetallics, 39 (2013) 11-19.

[24] M.P. Brady, J.L. Smialek, D.L. Humphrey, J. Smith, The role of Cr in promoting protective alumina scale formation by γ-based Ti-Al-Cr alloys— II. Oxidation behavior in air, Acta Materialia, 45 (1997) 2371-2382.

[25] G. Ghosh, Al-Fe-Ti (Aluminium - Iron - Titanium), in: G. Effenberg, S. Ilyenko (Eds.) Light Metal Systems. Part 2: Selected Systems from Al-Cu-Fe to Al-Fe-Ti, Springer Berlin Heidelberg, Berlin, Heidelberg, 2005, pp. 1-27.

[26] Y. Lu, J. Yamada, J. Nakamura, K. Yoshimi, H. Kato, Effect of B2-ordered phase on the deformation behavior of Ti-Mo-Al alloys at elevated temperature, Journal of Alloys and Compounds, 696 (2017) 130-135.

[27] H. Jiang, M. Hirohasi, Y. Lu, H. Imanari, Effect of Nb on the high temperature oxidation of Ti–(0–50 at.%)Al, Scripta Materialia, 46 (2002) 639-643.

[28] J. Shi, A. Zheng, Z. Lin, R. Chen, J. Zheng, Z. Cao, Effect of process control agent on alloying and mechanical behavior of L21 phase Ni–Ti–Al alloys, Materials Science and Engineering: A, 740-741 (2019) 130-136.

[29] M. Galano, F. Audebert, I.C. Stone, B. Cantor, Nanoquasicrystalline Al–Fe–Cr-based alloys. Part I: Phase transformations, Acta Materialia, 57 (2009) 5107-5119.

[30] A. Michalcová, D. Vojtěch, J. Čížek, I. Procházka, J. Drahokoupil, P. Novák, Microstructure characterization of rapidly solidified Al–Fe–Cr–Ce alloy by positron annihilation spectroscopy, Journal of Alloys and Compounds, 509 (2011) 3211-3218.

[31] A. Knaislová, P. Novák, J. Kopeček, F. Průša, Properties Comparison of Ti-Al-Si Alloys Produced by Various Metallurgy Methods, Materials, 12 (2019) 3084.

[32] P. Tsakiropoulos, On the Alloying and Properties of Tetragonal Nb_5Si_3 in Nb-Silicide Based Alloys, Materials, 11 (2018) 69.

[33] J. Zhang, H. Wang, F. Zhang, X. Lü, Y. Zhang, Q. Zhou, Growth kinetics and grain refinement mechanisms in an undercooled melt of a CoSi intermetallic compound, Journal of Alloys and Compounds, 781 (2019) 13-25.

[34] J. Pluhař, Nauka o materiálech, SNTL, 1989.

[35] X.T. Li, L.J. Huang, S. Jiang, Y.N. Gao, Q. An, S. Wang, R. Zhang, L. Geng, Microstructure and super oxidation resistance of the network structured Ti-Al-Si coating, Journal of Alloys and Compounds, 807 (2019) 151679.

[36] H. Hu, L. Huang, L. Geng, B. Liu, B. Wang, Oxidation behavior of TiB-whisker-reinforced Ti60 alloy composites with three-dimensional network architecture, Corrosion Science, 85 (2014) 7-14.

[37] Y. Jiao, L.J. Huang, S.L. Wei, L. Geng, M.F. Qian, S. Yue, Nano-Ti5Si3 leading to enhancement of oxidation resistance, Corrosion Science, 140 (2018) 223-230.

[38] B.V. Cockeram, R.A. Rapp, Oxidation-resistant boron- and germanium-doped silicide coatings for refractory metals at high temperature, Materials Science and Engineering: A, 192-193 (1995) 980-986.

[39] P. Novák, J. Kříž, A. Michalcová, D. Vojtěch, Microstructure Evolution of Fe-Al-Si and Ti-Al-Si Alloys during High-Temperature Oxidation, Materials Science Forum, 782 (2014) 353-358.

[40] P. Novák, J. Kříž, A. Michalcová, D. Vojtěch, Effect of alloying elements on properties of PM Ti-Al-Si alloys, Acta Metallurgica Slovaca, 19 (2013) 240-246.

[41] K.P. Rao, J.B. Zhou, Characterization of mechanically alloyed Ti–Al–Si powder blends and their subsequent thermal stability, Materials Science and Engineering: A, 338 (2002) 282-298.

[42] A. Vyas, K.P. Rao, Y.V.R.K. Prasad, Mechanical alloying characteristics and thermal stability of Ti–Al–Si and Ti–Al–Si–C powders, Journal of Alloys and Compounds, 475 (2009) 252-260.

[43] G. Liang, Q. Meng, Z. Li, E. Wang, Consolidation of nanocrystalline Al-Ti alloy powders synthesized by mechanical alloying, Nanostructured Materials, 5 (1995) 673-678.

[44] H.A. Calderon, V. Garibay-Febles, M. Umemoto, M. Yamaguchi, Mechanical properties of nanocrystalline Ti–Al–X alloys, Materials Science and Engineering: A, 329-331 (2002) 196-205.

[45] P. Haušild, M. Karlík, J. Čech, F. Průša, K. Nová, P. Novák, P. Minárik, J. Kopeček, Preparation of Fe-Al-Si Intermetallic Compound by Mechanical Alloying and Spark Plasma Sintering, Acta Physica Polonica A, 134 (2018).

[46] P. Novák, D. Vojtěch, J. Šerák, Wear and corrosion resistance of a plasma-nitrided PM tool steel alloyed with niobium, Surface and Coatings Technology, 200 (2006) 5229-5236.

[47] A. Knaislová, V. Šimůnková, P. Novák, High-temperature oxidation of intermetallics based on Ti-Al-Si system, Manufacturing Technology, 18 (2018) 255-258.

[48] P. Novák, F. Průša, J. Šerák, D. Vojtěch, A. Michalcová, High-temperature behaviour of Ti–Al–Si alloys produced by reactive sintering, Journal of Alloys and Compounds, 504 (2010) 320-324.

[49] K. Maki, M. Shioda, M. Sayashi, T. Shimizu, S. Isobe, Effect of silicon and niobium on oxidation resistance of TiAl intermetallics, in: S.H. Whang, D.P. Pope, C.T. Liu (Eds.) High Temperature Aluminides and Intermetallics, Elsevier, Oxford, 1992, pp. 591-596.

[50] H.-r. Jiang, Z.-l. Wang, W.-s. Ma, X.-r. Feng, Z.-q. Dong, L. Zhang, Y. Liu, Effects of Nb and Si on high temperature oxidation of TiAl, Transactions of Nonferrous Metals Society of China, 18 (2008) 512-517.

[51] M. Terner, S. Biamino, G. Baudana, A. Penna, P. Fino, M. Pavese, D. Ugues, C. Badini, Initial Oxidation Behavior in Air of TiAl-2Nb and TiAl-8Nb Alloys Produced by Electron Beam Melting, Journal of Materials Engineering and Performance, 24 (2015) 3982-3988.

[52] D. Vojtěch, J. Čížkovský, P. Novák, J. Šerák, T. Fabián, Effect of niobium on the structure and high-temperature oxidation of TiAl–Ti5Si3 eutectic alloy, Intermetallics, 16 (2008) 896-903.

[53] D. Vojtěch, T. Popela, J. Kubásek, J. Maixner, P. Novák, Comparison of Nb- and Ta-effectiveness for improvement of the cyclic oxidation resistance of TiAl-based intermetallics, Intermetallics, 19 (2011) 493-501.

[54] J.S. Wu, L.T. Zhang, F. Wang, K. Jiang, G.H. Qiu, The individual effects of niobium and silicon on the oxidation behaviour of Ti3Al based alloys, Intermetallics, 8 (2000) 19-28.

Figure and table captions

Fig. 1 XRD patterns of TiAl15Si15X15 powders

Fig. 2 Scanning electron micrographs and local chemical analysis (EDS, in at. %) of TiAl15Si15X15 (X = Co, Cr, Fe, Mo, Nb, Ni) powders prepared by mechanical alloying

Fig. 3 XRD patterns of TiAl15Si15X15 compact alloys

Fig. 4 Scanning electron micrographs and local chemical analysis (EDS, in at. %) of TiAl15Si15X15 (X = Co, Cr, Fe, Mo, Nb, Ni) alloys prepared by mechanical alloying and Spark Plasma Sintering

Fig. 5 Porosity and pore size of TiAl15Si15X15 compact alloys

Fig. 6 Microhardness of TiAl15Si15X15 compact alloys

Fig. 7 Fracture toughness of TiAl15Si15X15 compact alloys

Fig. 8 Abrasive wear resistance of TiAl15Si15X15 compact alloys

Fig. 9 Time dependence of the Ti–Al–Si-X alloys (MA+SPS) mass gain during cyclic oxidation at 800 °C

Fig. 10 Time dependence of the scaled-off oxides (MA+SPS) mass gain during cyclic oxidation at 800 °C

Fig. 11 Appearance of Ti–Al–Si-X alloys (MA+SPS) after 400 h of cyclic oxidation at 800 °C: a) TiAl15Si15Co15, b) TiAl15Si15Cr15, c) TiAl15Si15Fe15, d) TiAl15Si15Mo15, e) TiAl15Si15Nb15, f) TiAl15Si15Ni15

Fig. 12 Time dependence of the Ti–Al–Si-X alloys (MA+SPS) mass gain during cyclic oxidation at 1000 °C

Fig. 13 Time dependence of the scaled-off oxides (MA+SPS) mass gain during cyclic oxidation at 1000 °C

Fig. 14 Appearance of Ti–Al–Si-X alloys (MA+SPS) after 400 h of cyclic oxidation at 1000 °C: a) TiAl15Si15Co15, b) TiAl15Si15Cr15, c) TiAl15Si15Fe15, d) TiAl15Si15Mo15, e) TiAl15Si15Nb15, f) TiAl15Si15Ni15

Fig. 15 Microstructure (SEM) of the Ti–Al–Si-X alloys (MA+SPS) after cyclic oxidation (400 h): a) TiAl15Si15Co15, b) TiAl15Si15Cr15, c) TiAl15Si15Fe15

Fig. 16 Microstructure (SEM) of the Ti–Al–Si-X alloys (MA+SPS) after cyclic oxidation (400 h): a) TiAl15Si15Mo15, b) TiAl15Si15Nb15, c) TiAl15Si15Ni15

Table 1 Ultimate compression strength values of Ti-Al-Si-X alloys

Table 2 Phase composition of the surface oxide layer of Ti-Al-Si-X alloys after 400 hours of cyclic oxidation